L. MERRILL

HIGH PRESSURE, HIGH TEMPERATURE SYNTHESES OF RARE EARTH DIANTIMONIDES AND Th_3P_4 TYPE POLYMORPHS OF RARE EARTH SESQUISULFIDES

A Dissertation

Presented to the

Department of Chemistry

Brigham Young University

In Partial Fulfillment

of the Requirements for the Degree

Doctor of Philosophy

by

Norman L. Eatough

August 1968

HIGH PRESSURE, HIGH TEMPERATURE SYNTHESES OF RARE EARTH DIANTIMONIDES AND Th_3P_4 TYPE POLYMORPHS OF RARE EARTH SESQUISULFIDES

A Dissertation

Presented to the

Department of Chemistry

Brigham Young University

In Partial Fulfillment

of the Requirements for the Degree

Doctor of Philosophy

by

Norman L. Eatough

August 1968

TABLE OF CONTENTS

This dissertation, by Norman L. Eatough is accepted in its present form by the Department of Chemistry of Brigham Young University as satisfying the dissertation requirement for the degree Doctor of Philosophy.

Date

Chairman, Advisory Committee

Member, Advisory Committee

Member, Advisory Committee

Chairman, Major Department

LIST OF TABLES

LIST OF FIGURES

LIST OF FIGURES

(CONTINUED)

ACKNOWLEDGEMENTS

Thanks is gratefully given to Dr. H. T. Hall who directed this research. I wish to acknowledge the debt of friendship I have to John Cannon, Jim Hoen, Dr. M. D. Horton, Karl Miller and Alan Webb who gave needed, if not always welcome, help on many of the problems associated with this research. Special thanks is given to Alan Webb who furnished the computer programs used in the X ray diffraction work.

I acknowledge the support of an NSF traineeship which took the financial worry out of my graduate work. This work was commenced on an NSF grant to Dr. H. T. Hall and completed on a U. S. Army Research Office, Durham, grant to him. Thanks is given for this support. I also wish to acknowledge general support of the BYU High Pressure Laboratory by the BYU Research Division.

This work is dedicated to my wonderful wife, Marilyn, and our children; LaRae, Craig, Steven and Jerry. Their love and faith in me have been an ever present and much needed source of encouragement and support.

I. INTRODUCTION

The problem selected for high pressure, high temperature synthesis studies was the extension of the rare earth diantimonide and cubic rare earth sesquisulfide series of compounds. Since diantimonides and cubic sesquisulfides of the light rare earth elements are known (1),(2) it seemed probable the other compounds of these series could be formed by the proper application of high pressure, high temperature techniques.

Series of compounds which are found over a given range and then do not exist for the rest of the elements are common in compounds of the lanthanide elements. A listing of the lanthanide elements and their atomic numbers is given in Table 1.

TABLE 1

THE LANTHANIDE ELEMENTS AND THEIR ATOMIC NUMBERS

Sc														
21														
Y														
39														
La	Ce	Pr	Nd	Pm	Sm	Eu	Gd	Tb	Dy	Ho	Er	Tm	Yb	Lu
57	58	59	60	61	62	63	64	65	66	67	68	69	70	71

This discontinuity has usually been attributed to instability of bonding or of the crystal structure because of size differences from the lanthanide contraction. It seemed reasonable that the application of very high pressure might force the elements close enough to allow bonding to occur that would not be possible under ordinary pressures. It was hoped that these bonds would remain stable or at least metastable after the pressure was released.

Recent studies on rare earth antimony compounds have provided a convenient test for this hypothesis (1). The RSb_2 compounds, where R is a rare earth metal, exist in an orthorhombic crystal structure from La to Sm but the diantimonides of Gd to Ho could not be synthesized by the ordinary high vacuum techniques. It seemed worthwhile to see if high pressure, high temperature techniques could extend the series into the unknown region.

The syntheses were carried out in a tetrahedral anvil press at pressures up to 70 kilobars and temperatures to 1800 °C. The known orthorhombic structure was extended two elements to $GdSb_2$ and $TbSb_2$. A different type structure was obtained which could also be indexed as orthorhombic for $GdSb_2$, $TbSb_2$, $DySb_2$, $HoSb_2$, $ErSb_2$, $TmSb_2$ and YSb_2. No diantimonides of La, Ce, Eu or Lu could be synthesized.

The rare earth sesquioxides have long been known in both cubic and a more dense monoclinic form. The cubic

form was known for all the R_2O_3 compounds but the monoclinic form was known only for the lighter elements from La to Dy. The heavy element sesquioxides were converted from the cubic form to the monoclinic modification by application of high pressure, high temperature techniques by Hoekstra (3).

The only other rare earth series which have been studied under high pressure, high temperature conditions are the monotellurides by Rooymans (4) and a study on the phosphates, arsenates, vanadates, tantalates and niobates by Stubican and Roy (5). New polymorphs of known compounds were found in both of these studies.

An examination of crystal structure and density data for rare earth sesquisulfides (2), (6) showed that the monoclinic form was known for all the rare earths but in this case the cubic form was more dense and was known only for the lighter elements La through Dy. Also the coordination number of eight in the cubic form is higher than the six coordinated monoclinic form (7).

Since high pressure favors the more dense and higher coordinated structure it seemed probable that the conversion from monoclinic to the cubic form could be carried out for the heavy rare earths by application of high pressure, high temperature techniques. In the present work the monoclinic form of Ho_2S_3, Er_2S_3, Tm_2S_3 and Y_2S_3 were all converted to the Th_3P_4 type cubic structure at about 75 kilobars and 2000 °C. Orthorhombic Yb_2S_3 was also

converted to the cubic form under these conditions. Rhobohedral Lu_2S_3 was partially converted to the cubic form under these conditions.

It is interesting to note that Gschneidner has published a chart which lists the known RB and RB_2 type compounds where R is a rare earth element and B is any other element (8). The chart shows several other series that could be extended by the high pressure techniques used in this study.

II. LITERATURE REVIEW

Rare Earth Diantimonides

All of the rare earth monoantimonides are known and have been studied extensively because of their semiconductor properties. Brixner has summarized the crystallographic data for these compounds except for EuSb and LuSb (9). They all exist in only the NaCl cubic structure. EuSb was prepared by Bruzzone(10) and LuSb by Przybylska (11) and Iandelli (12).

Three rare earth - antimony systems have been studied quite extensively and phase diagrams have been prepared for them. In 1954 Vogel and Klose studied the La-Sb system and found the compounds La_2Sb, La_3Sb_2, LaSb and $LaSb_2$ (13). This was the first rare earth diantimonide reported. In 1966 Olcese found Ce_2Sb, Ce_3Sb_2, CeSb and $CeSb_2$ by X ray examination of the Ce-Sb system (14). In 1967 Bodnar and Steinfink studied the Yb-Sb system and reported the compounds: $YbSb_2$, YbSb, Yb_5Sb_4, Yb_4Sb_3, Yb_5Sb_3 and Yb_5Sb_2 (15).

In 1966 Hohnke and Parthe reported the synthesis of R_4Sb_3 type compounds where R was La, Ce, Pr, Nd, Gd, Tb, Dy, Ho or Yb (16). These compounds were cubic with the anti

Th_3P_4 type structure. In 1967 Gambino reported that this structure was stable for elements La to Dy but rare earths heavier than Dy would not form R_4Sb_3 type compounds (17).

A study specifically on rare earth diantimonides was reported by Wang and Steinfink in 1967 (1). They prepared $LaSb_2$, $CeSb_2$, $NdSb_2$, $SmSb_2$, and $YbSb_2$. They attempted to synthesize $GdSb_2$, $DySb_2$, $HoSb_2$, and $ErSb_2$ but were not successful. They did not work with Pr, Eu, Tb, Tm, or Lu. Through single crystal X ray diffraction work the compounds prepared were shown to have an orthorhombic structure which they call the $LaSb_2$ type structure. By detailed analysis of the cell structure they found the structure has a very short Sb-Sb bond and postulated that as the rare earth size decreases it forces the critical Sb-Sb distance to become shorter and Sb-Sb repulsion finally causes the structure to become unstable at Gd.

It seemed reasonable to expect that very high pressure would force the antimony atoms closer together and allow bonding to take place which could result in a stable or at least metastable compound. This was the genesis of the present work.

Rare Earth Sesquisulfides

Studies of the crystal chemistry of the rare earth metal sulfides have shown that the lighter elements from La to Dy have sesquisulfides with a Th_3P_4 type cubic

structure with the exception of Eu_2S_3 which does not exist (2), (6). The elements from La to Sm also form a series of compounds R_3S_4 with the same Th_3P_4 type cubic structure.

The R_3S_4 and R_2S_3 structures are the same except R_2S_3 has 1 1/3 rare earth metal vacancies per unit cell compared to R_3S_4, therefore no change in lattice parameter is found between the two types. This means there is a range of homogeniety R_2S_3 to R_3S_4 with no change in diffraction pattern so that X ray diffraction analysis can not be used to differentiate between the two types of compounds. There is, however, a considerable difference in density between the two structures. This effect has been observed for the lighter rare earths from La to Sm (2). Interestingly Eu_3S_4 is known but Eu_2S_3 does not exist (2). For the heavier rare earths of Gd, Tb and Dy the range of homogeniety is not observed and the R_3S_4 compounds do not exist for these rare earths (2), (6).

Guittard has shown that a range of NaCl type cubic homogeniety is found in the metal rich sulfides from RS to R_4S_3 for the heavy lanthanides from Tb to Tm. For Lu the NaCl type homogeniety is found from LuS to Lu_3S_4 but does not include Lu_2S_3 (18). Cutler has shown that the R_3S_4 compounds are metallic conductors while the R_2S_3 compounds are semiconductors or insulators. The rare earth furnishes electrons to the conduction band when it is present at a ratio higher than is necessary to satisfy the valence

requirements of sulfur (19).

The sesquisulfide, Dy_2S_3, is found in a monoclinic form as well as the Th_3P_4 cubic structure. The heavier rare earths Ho to Tm have only monoclinic sesquisulfides (2), (6). Y_2S_3 is also found only in the monoclinic form (20) while Yb_2S_3 exists in a rhombohedral form as well as an orthorhombic modification (21), (22). Lu_2S_3 is known only in a rhombohedral form (22). The orthorhombic Yb_2S_3 displays homogeniety from Yb_2S_3 to Yb_3S_4 (21).

The work discussed above shows that a change of structure is observed in the rare earth sesquisulfides at Dy_2S_3. Compounds of lighter lanthanides exist in a cubic form and compounds of heavier elements exist in a monoclinic, orthorhombic or rhombohedral structure. Since the cubic form is considerably more dense than the monoclinic form and has a higher coordination number (eight for the rare earth metal in the cubic form and six in the monoclinic) it seemed very probable that the monoclinic form could be converted to the cubic form using high pressure techniques. Part of the present work was performed to determine if this could be done.

Densities of the monoclinic, orthorhombic, rhombohedral and cubic forms of the rare earth sesquisulfides (2), (6), (21) which served as the basis for predicting that the transformations could be carried are shown in Figure 1.

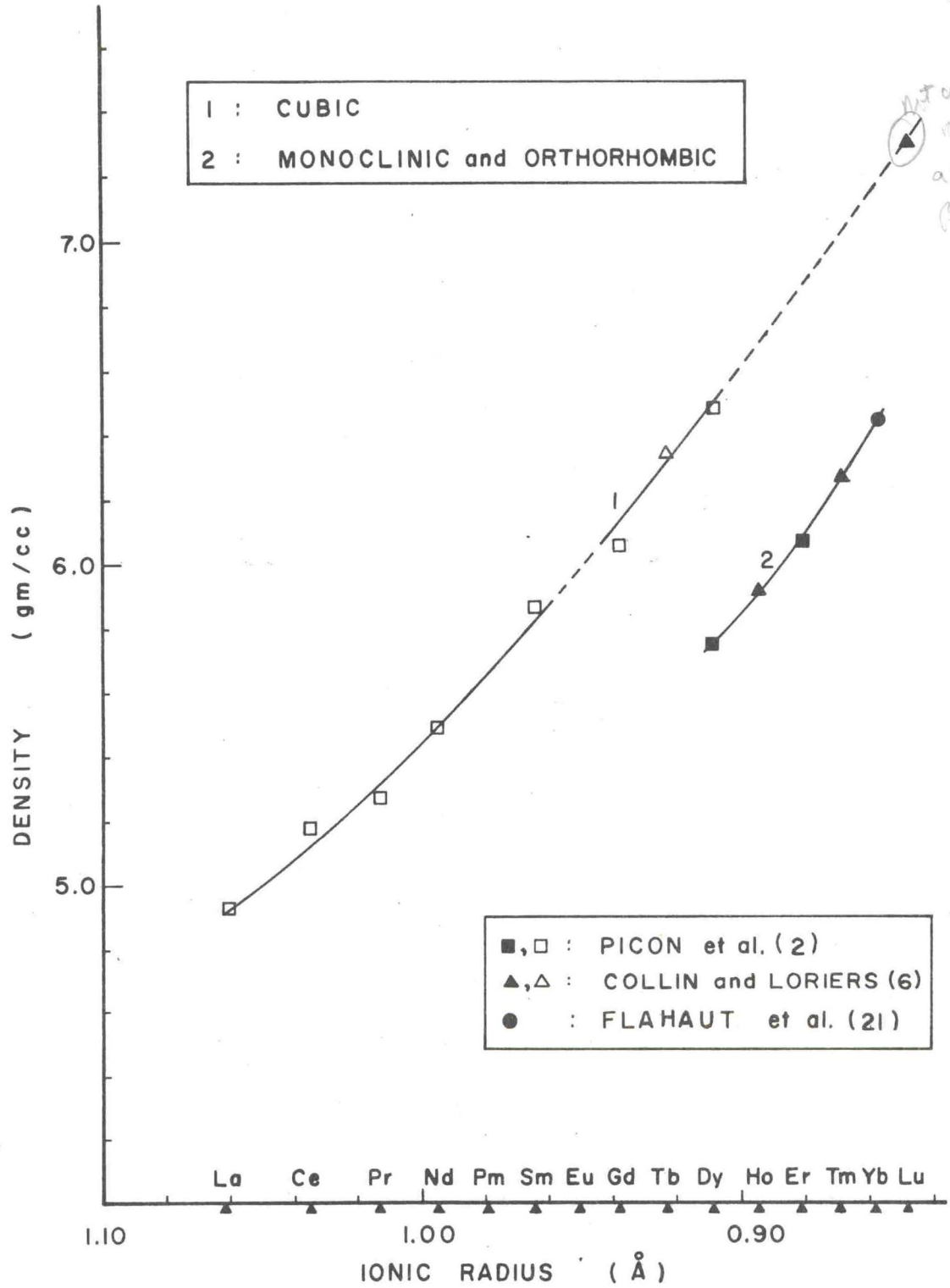

Fig. 1.--Densities of Rare Earth Sesquisulfides.

III. APPARATUS

The high pressure studies of the rare earth diantimonides were carried out in the tetrahedral anvil apparatus, T-2, at Brigham Young University designed by Dr. H. T. Hall (23), (24). With 3/4 inch anvils this press is capable of generating 70 kilobars and 2000 ^{o}C in the sample geometry used.

The press consists of four 200 ton hydraulic rams driven along lines normal to the faces of a tetrahedron by an air-actuated pump. Cemented tungsten carbide anvils with 3/4 inch triangular faces are mounted in steel binding rings and are aligned by an anvil guide device. The anvils press against the face of a one-inch tetrahedron made of pyrophyllite, a hydrated alumina silicate, in which the sample is contained. The pyrophyllite tetrahedron is 25 per cent larger than the tetrahedron outlined by the anvil faces so that a gasket of extruded pyrophyllite will be formed as the anvils are advanced. The pyrophyllite has a high internal friction but is compressible so it contains the sample inside the tetrahedron and the gasket still allows compression and consequential pressure generation on the sample.

The press and control panel are shown in Figure 2

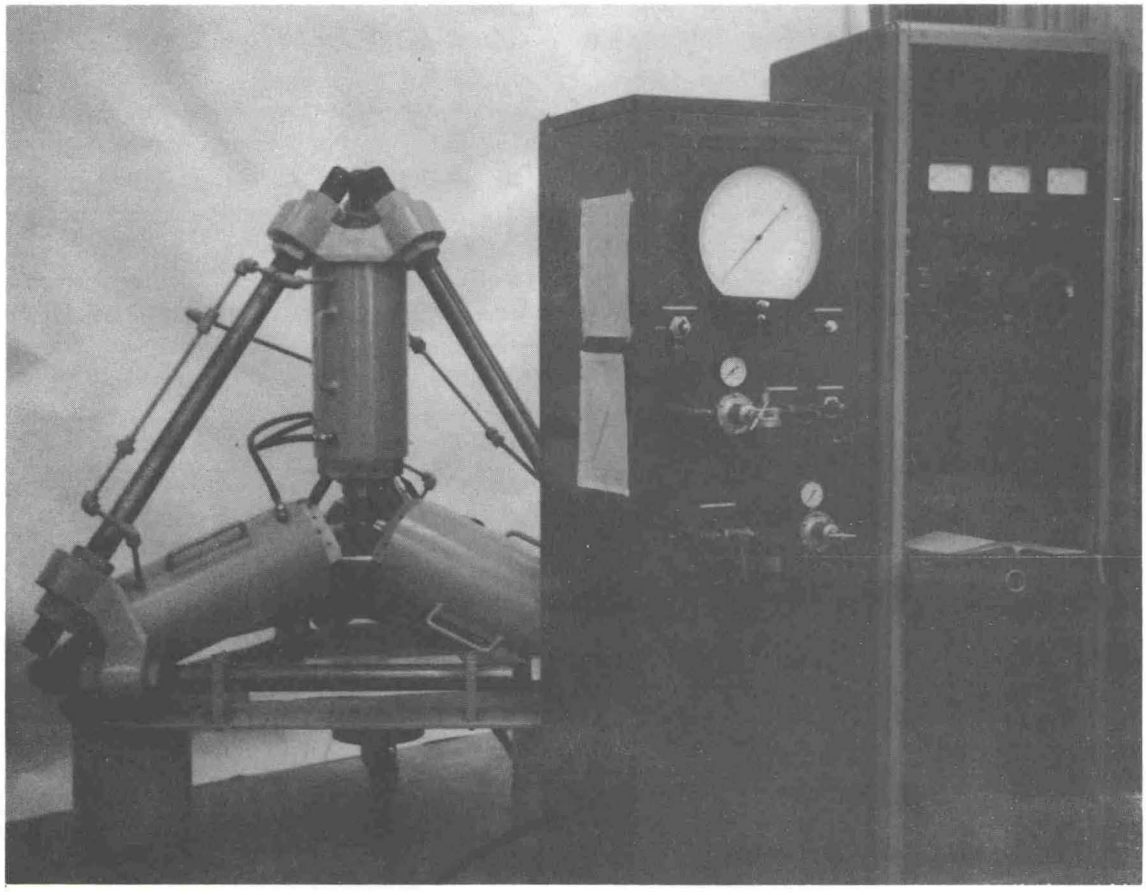

Fig. 2.--Tetrahedral Press and Control Panel

and the tetrahedral sample assembly is shown in Figure 3.

The tetrahedrons were made of American Grade A Lava (pyrophyllite) and had one-inch edges and a 0.125 inch sample hole. The electrical leads were made from pieces of molybdenum 0.50 by 0.22 by 0.005 inches. The graphite heater consisted of a tube 0.125 inch O.D. by 0.085 inch I.D. by 0.15 inch long and two end caps 0.125 inch diameter by 0.050 inch thick. The boron nitride liner fit inside the graphite tube and was made of a tube 0.085 inch O.D. by 0.050 inch I.D. by 0.10 inch long and two end caps 0.085 inch diameter by 0.020 inch thick. The reagents for synthesis were placed inside the BN tube.

In order to provide a larger sample volume for metallographic studies and density determinations the BN liner was replaced by a molybdenum tube formed from a piece of Mo 0.20 by 0.30 by 0.002 inches and two Mo end caps 0.125 inch diameter by 0.005 inch thick. The graphite heater was a tube 0.125 inch O.D. by 0.085 inch I.D. by 0.20 inch long and two end caps 0.125 inch diameter by 0.020 inch thick.

The studies on the rare earth sesquisulfides were carried out in a cubic anvil press, C-2, using 1/2-inch WC anvils. This press is similar to the tetrahedral press except it has six rams directed normal to the faces of a cube. A pyrophyllite cube was used to hold the sample and form the compressible gasket. The cubic sample assembly is shown in Figure 4.

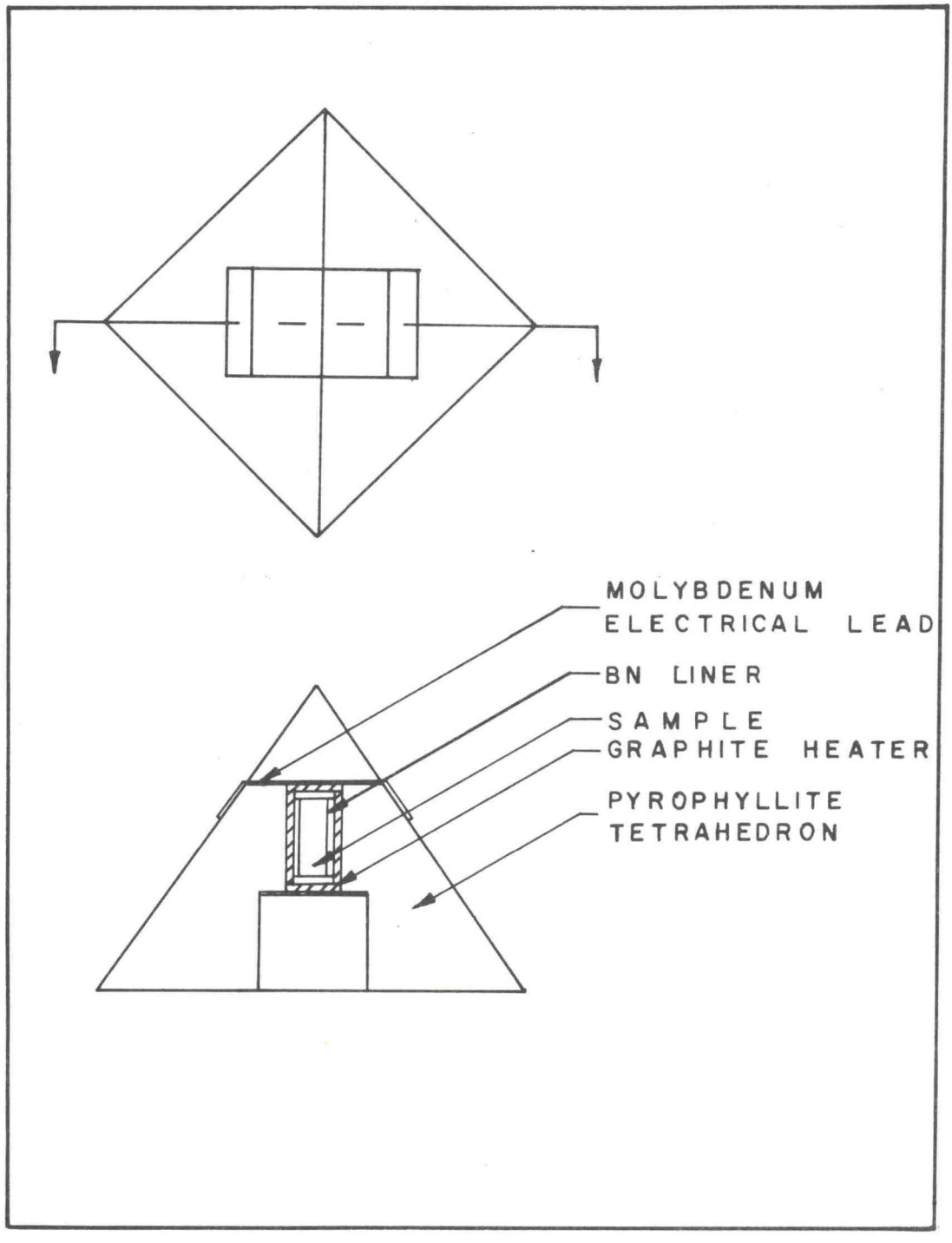

Figure 3.-Tetrahedral Sample Assembly

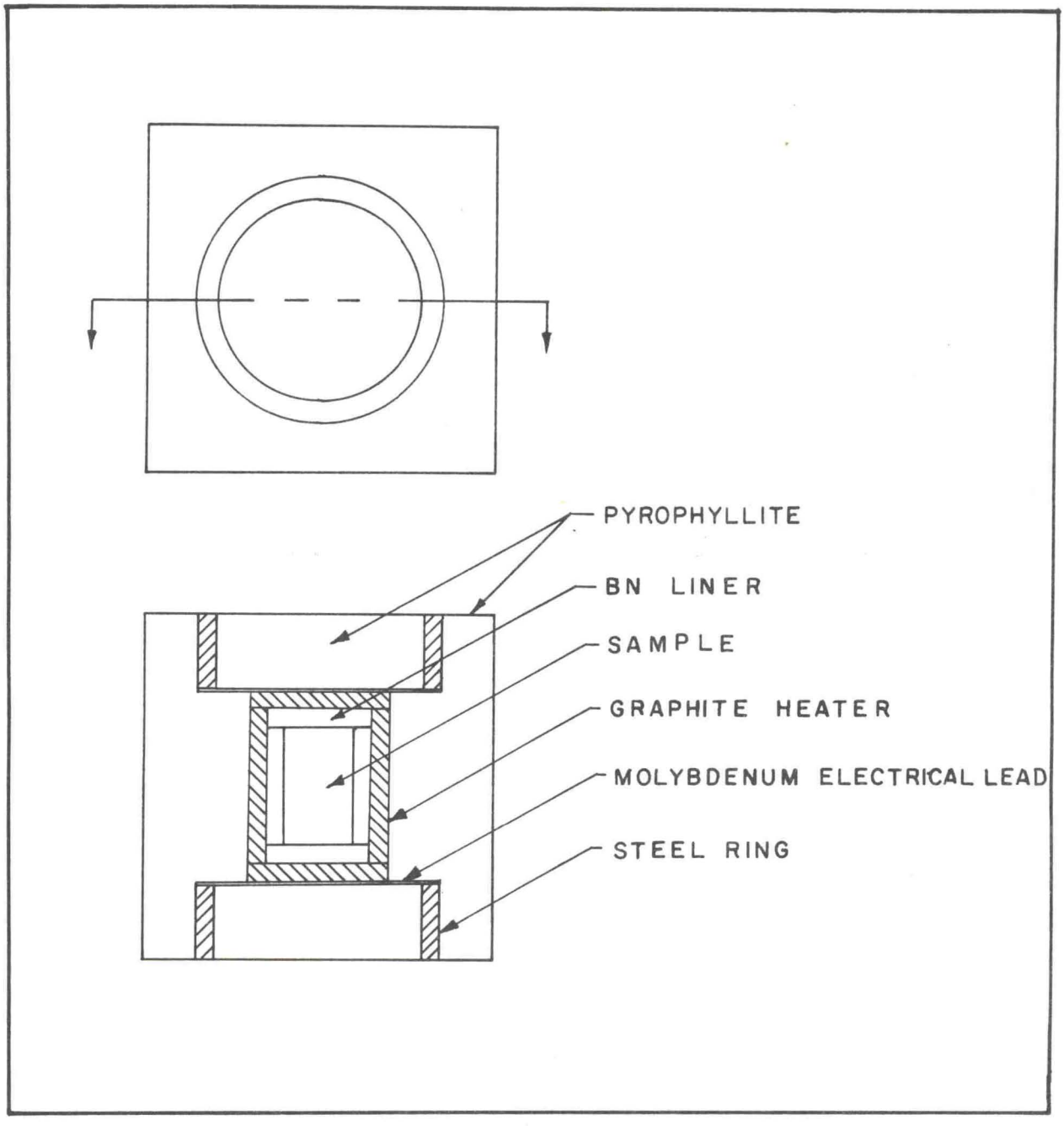

Figure 4.-Cubic Sample Assembly

The steel ring, 0.30 inch O.D. by 0.20 inch I.D. by 0.10 inch thick served as an electrical connection between the graphite heater and the anvils. The heater was a graphite tube 0.155 inch O.D. by 0.115 inch I.D. by 0.22 inch long and two end caps 0.155 inch diameter by 0.030 inch thick. The BN liner was a tube 0.115 inch O. D. by 0.075 inch I.D. by 0.16 inch long and two end caps 0.115 inch diameter by 0.030 inch thick. The sample was packed inside the BN liner.

IV. SYNTHESES STUDIES OF RARE EARTH DIANTIMONIDES

Syntheses studies were carried out on all of the lanthanides except Pm and also on Sc and Y.

The rare earth metals were obtained from Research Chemicals of Phoenix, Arizona and Alfa Inorganics of Beverly, Massachusetts and were 99.9 per cent pure. The antimony was obtained from Mallinckrodt Chemical Works of New York and was 99.8 per cent pure, reagent grade metal. The rare earths were filed and the filings sieved through a 100 mesh nylon sieve and used immediately. The antimony was ground with a mortar and pestle and sieved through a 200 mesh nylon sieve. Mixtures of one mole rare earth to two moles of antimony were prepared and hand mixed for several minutes in a plastic vial.

The pyrophyllite tetrahedrons were prepared as shown in Figure 3 and the sample loaded in the BN tube. The sample was compressed by hand with a metal tamp and the completed tetrahedron painted with a slurry of rouge in methanol, dried at 110 ^{o}C for at least one hour and allowed to cool in a dessicator.

The completed sample was placed in the press and compressed to the desired pressure. The power was raised to the desired wattage over about fifteen seconds and held

at that wattage for three minutes. The sample was quenched by shutting off the power and allowed to remain at pressure for one minute longer after which the pressure was released over about a thirty second period.

The sample was removed from the BN tube, crushed between two polished WC anvils, loaded in an X ray capillary tube and an X ray diffraction pattern taken at once.

Runs were made from pressures of 15 to 70 kilobars. Temperatures of 600 to 1000 °C were used at the lower pressures and 600 to 1800 °C at the higher pressures. Enough runs were made for each system to define the reaction product boundaries. The boundaries were defined to ± 3 kilobars and about ± 100 °C. Reaction products were identified by their X ray powder diffraction patterns.

The results obtained from each system are summarized in Table 2 and shown in Figures 5 through 11.

Lanthanum

Only La_2O_3 + Sb were obtained from 40 to 60 kilobars for temperatures above 1000 °C. At lower temperatures there was no reaction. The oxygen apparently migrated into the sample from the pyrophyllite.

Cerium

Only CeO_2 + Sb were obtained from 20 to 65 kilobars for temperatures up to 900 °C. At higher temperatures Ce_2O_3 + Sb were obtained.

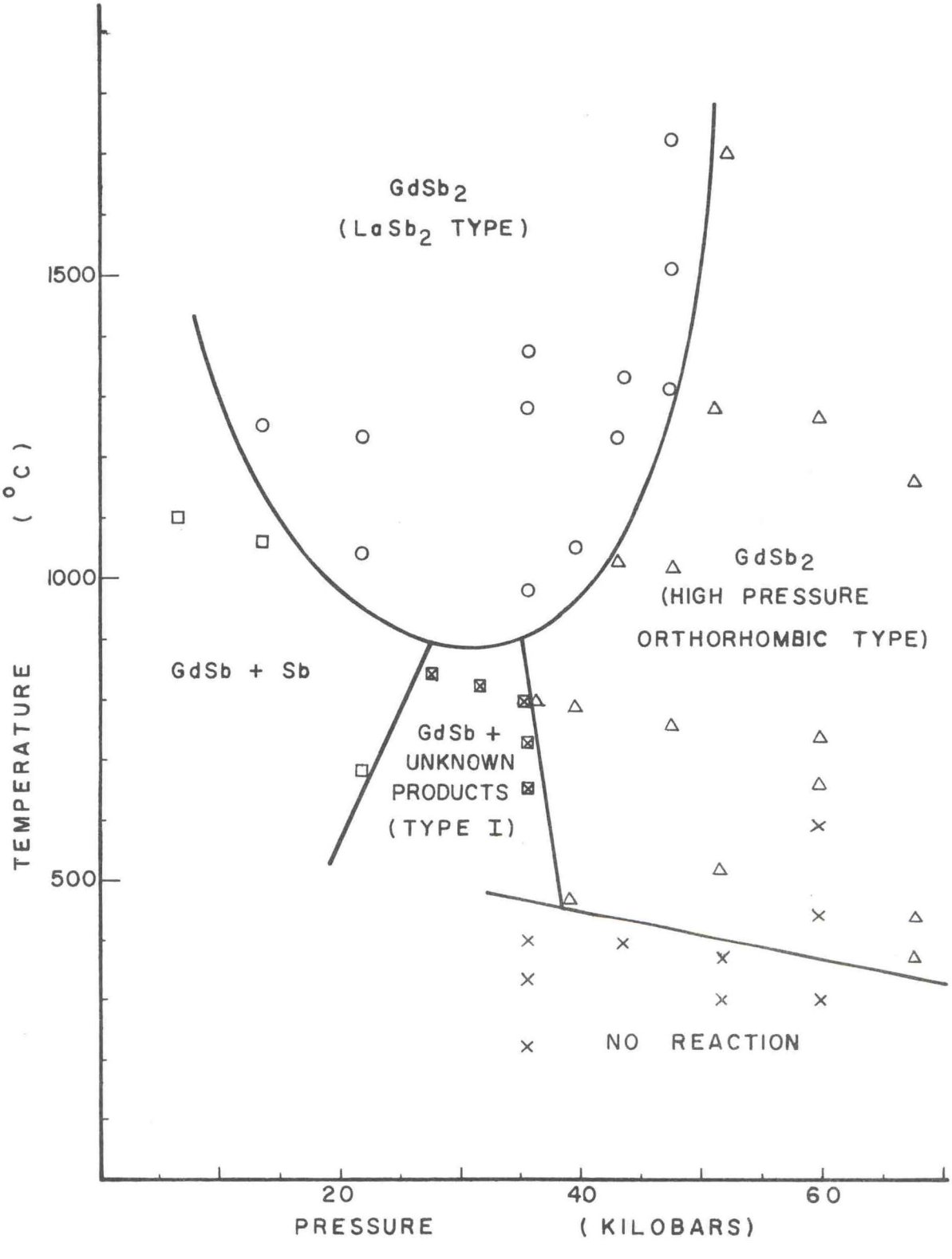

Fig.5.--Gd + 2 Sb Reaction Product Diagram.

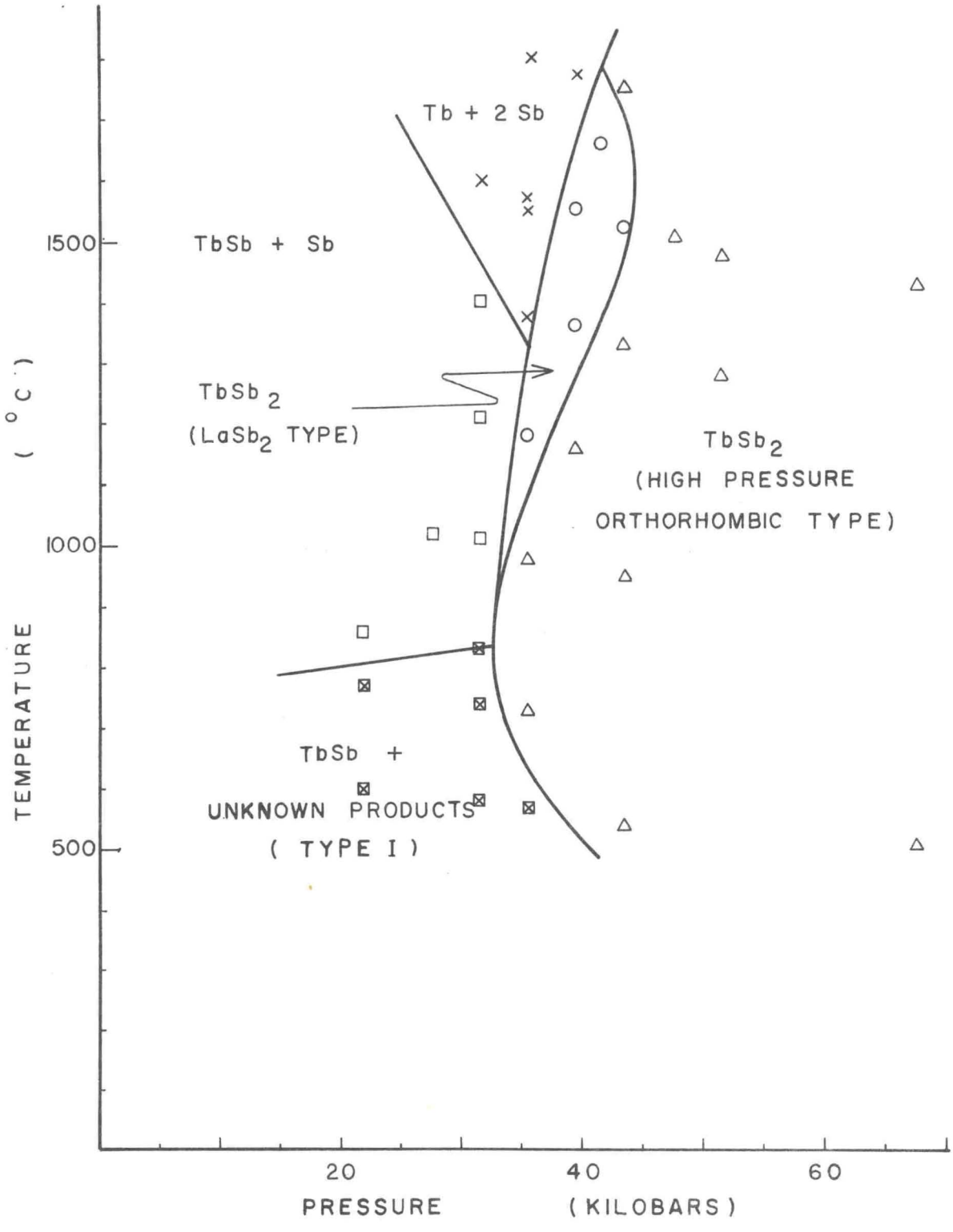

Fig. 6.--Tb + 2 Sb Reaction Product Diagram.

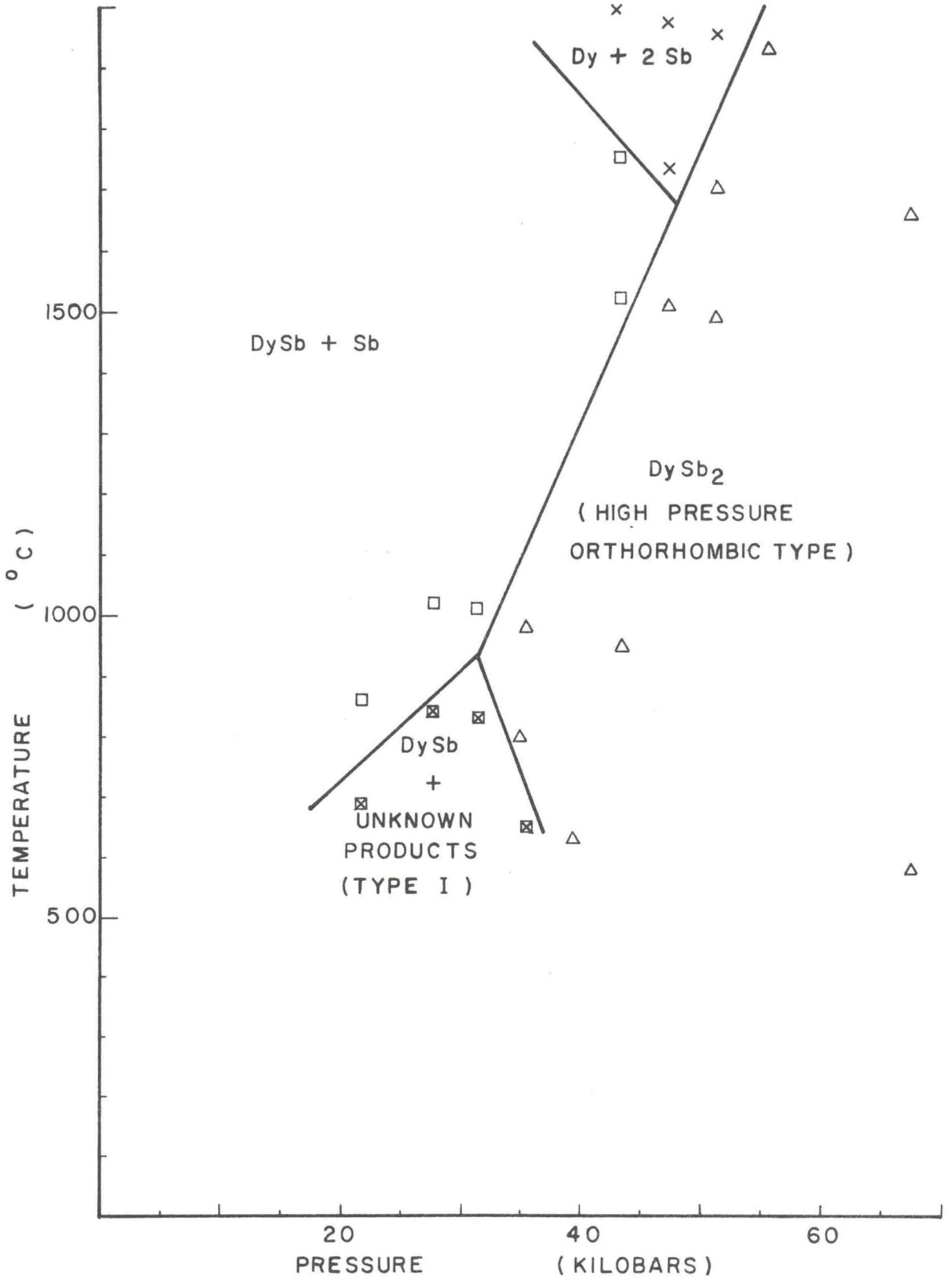

Fig. 7.--Dy + 2 Sb Reaction Product Diagram.

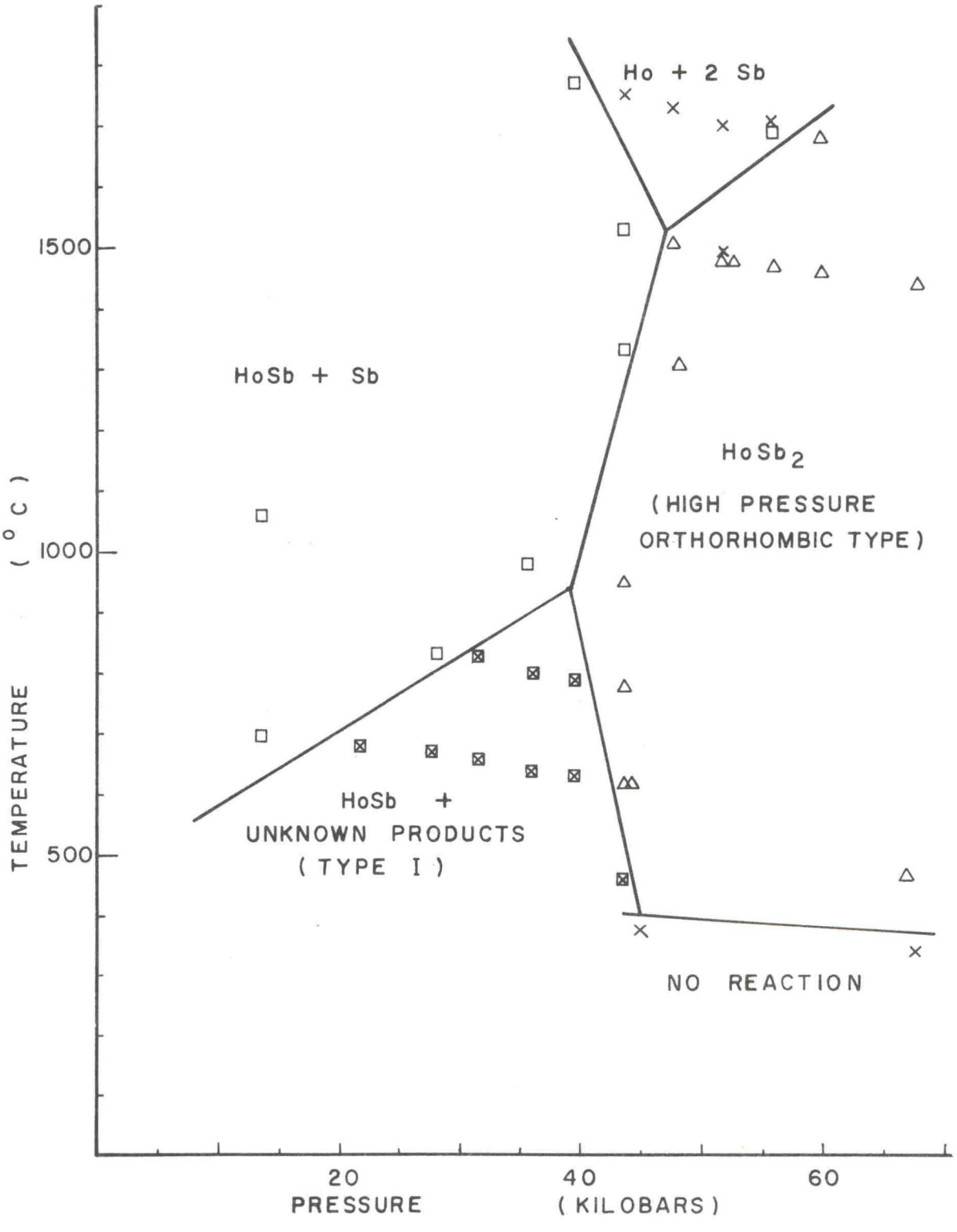

Fig. 8.--Ho + 2 Sb Reaction Produdt Diagram.

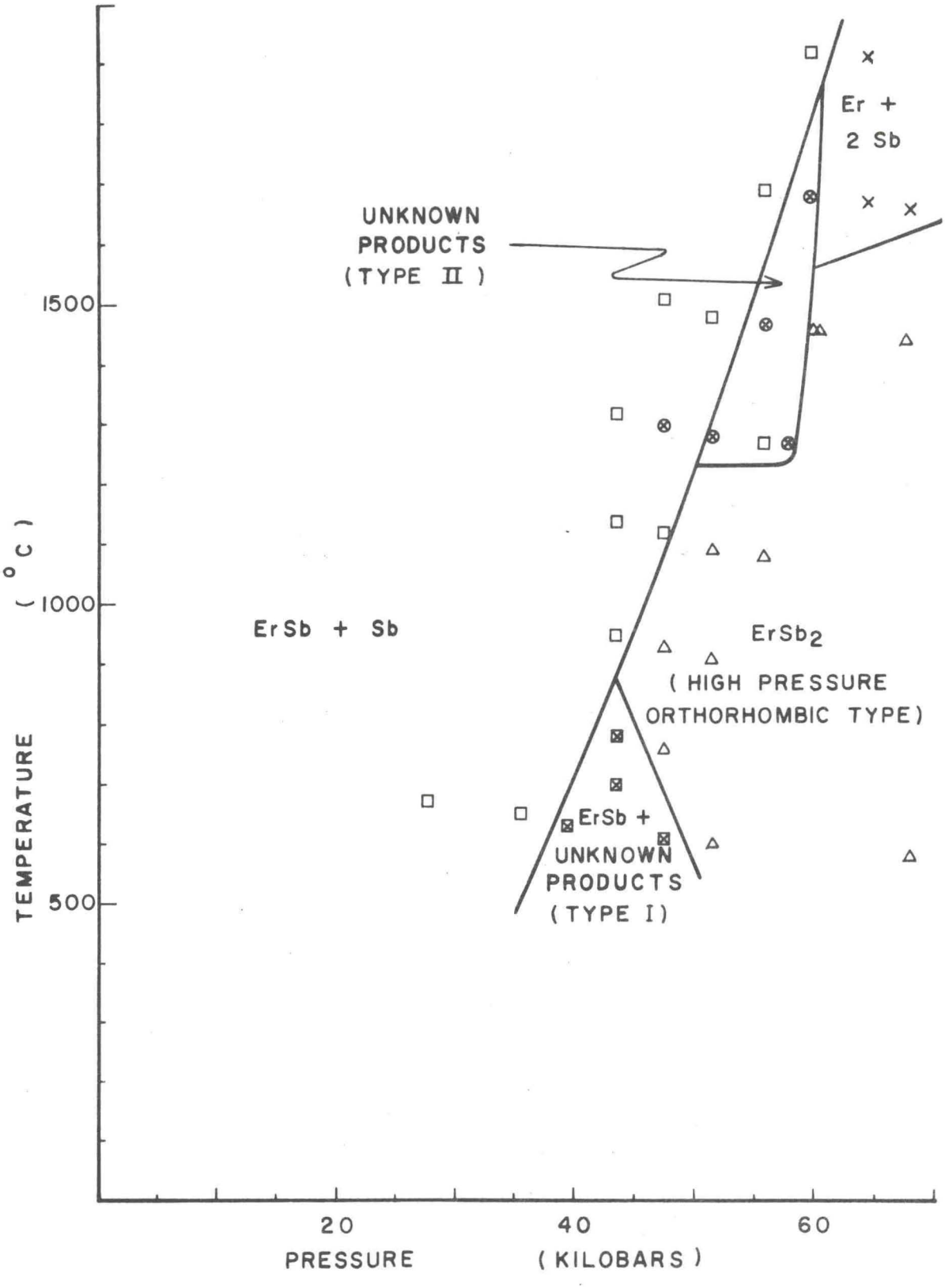

Fig 9.--Er + 2 Sb Reaction Product Diagram.

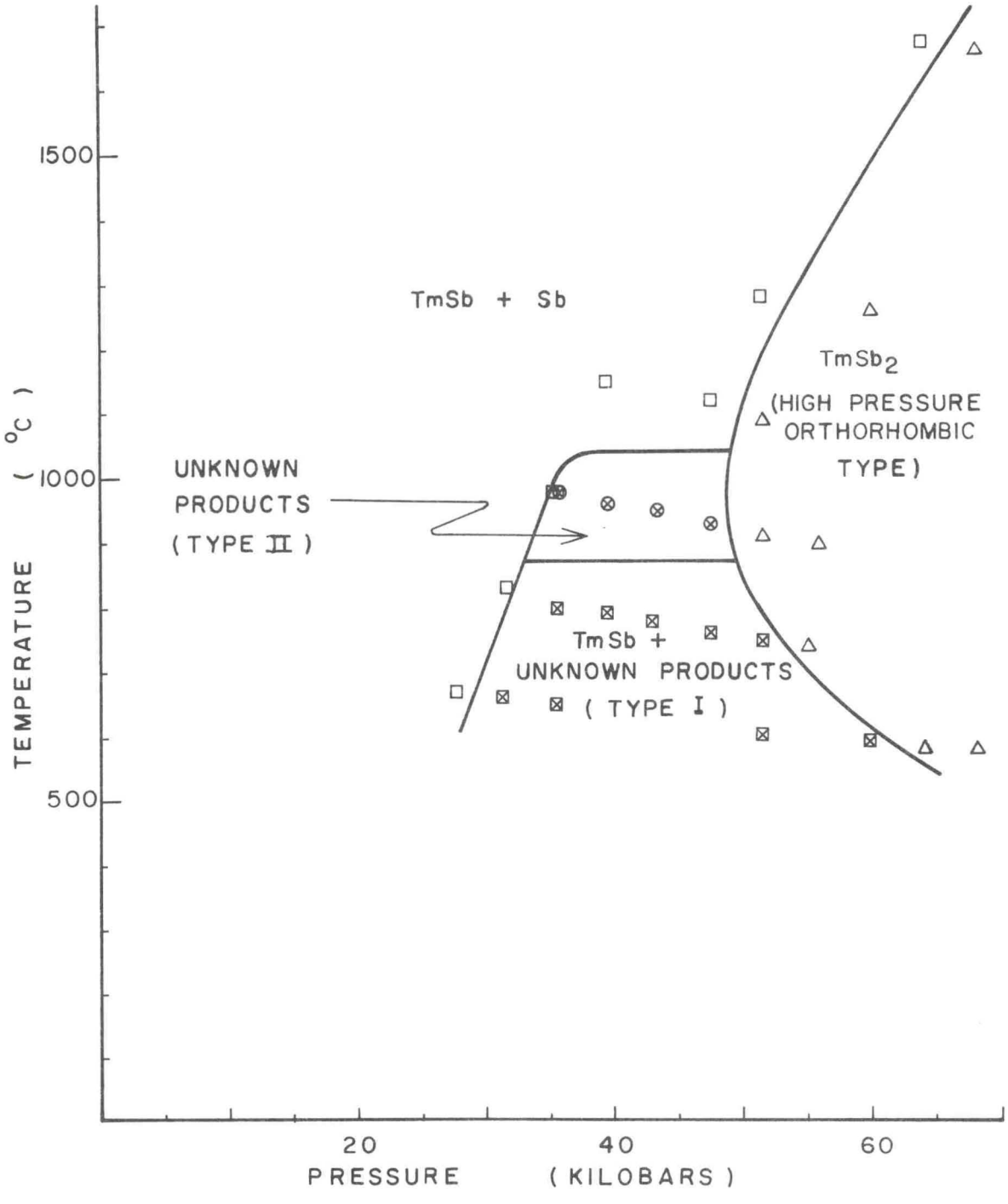

Fig 10.--Tm + 2 Sb Reaction Product Diagram.

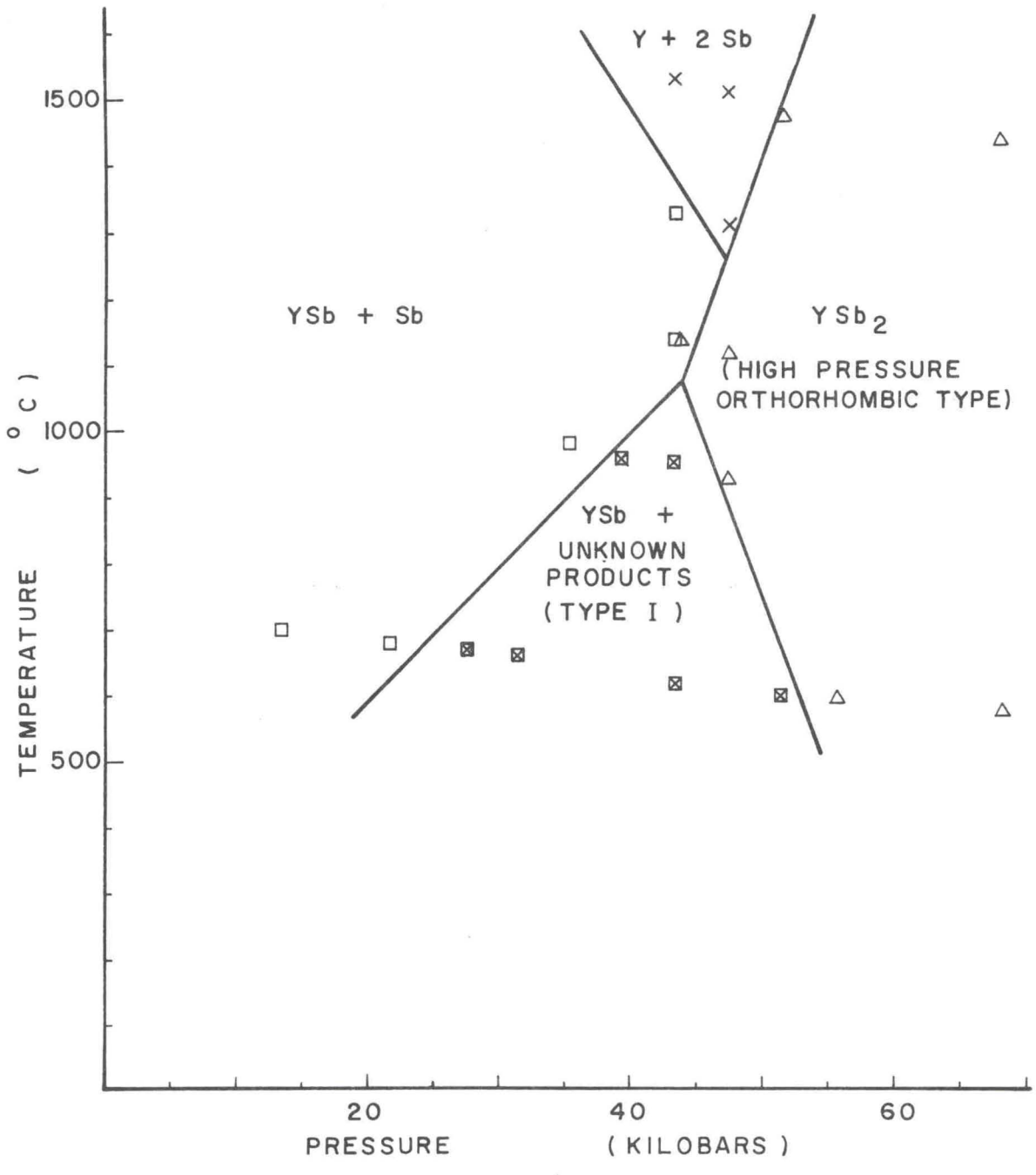

Fig 11.--Y + 2 Sb Reaction Product Diagram.

Praseodymium

Above about 600 °C at all pressures up to 70 kilobars a compound was formed whose X ray diffraction pattern could be matched line for line to the $LaSb_2$ type orthorhombic pattern for $NdSb_2$ given by Wang (25). It was concluded that $PrSb_2$ had been synthesized. This compound had not been reported previously. No other reaction products were observed.

Neodymium

Only $LaSb_2$ type $NdSb_2$ was observed above 600 °C for all pressures up to 70 kilobars. $NdSb_2$ was identified by comparing its X ray powder diffraction pattern with the pattern given by Wang (25).

Samarium

Only $LaSb_2$ type $SmSb_2$ was obtained above 600 °C for all pressures up to 70 kilobars.

Europium

A white or yellow powder plus antimony was obtained for all conditions above 400 °C and up to 70 kilobars. The powder was not definitely identified but was probably a europium oxide.

Gadolinium

Several different reaction products were obtained in this case. The reaction product diagram is shown in Figure

5. At pressures between 10 and 50 kilobars and temperatures above 1000 °C an X ray diffraction pattern which matched that of $NdSb_2$ was obtained which verified the synthesis of $LaSb_2$ type $GdSb_2$, a new compound. At lower temperatures and pressures below 20 kilobars cubic GdSb plus Sb were obtained. At temperatures below 900 °C and pressures between 25 and 35 kilobars a mixture of GdSb and unidentified products was obtained. The cubic lines of GdSb could easily be picked out of the X ray diffraction pattern but there were several additional weak lines which were not identified. This phase was called "unknown product, type I". At pressures above 40 to 50 kilobars and temperatures high enough to obtain reaction, a new phase was observed. The X ray diffraction pattern of this phase could be indexed with an orthorhombic structure containing two molecules per unit cell. This orthorhombic structure is quite different from the $LaSb_2$ type reported for rare earth diantimonides by Wang and Steinfink (1). This structure was called the "high pressure orthorhombic" phase.

Different mixture ratios of Gd plus Sb were prepared and used to see if this high pressure orthorhombic phase was a compound or a solid solution. For an equimolar mixture of Gd plus Sb only GdSb was formed at 60 kilobars and 1100 °C. For a 2 to 3 molar mixture of Gd plus Sb, the high pressure orthorhombic structure was observed with the same lattice parameters as found in the 1 to 2 molar runs.

For a 1 to 3 molar mixture of Gd plus Sb the same high pressure orthorhombic structure was observed at these conditions along with excess antimony lines. Again there was no change in lattice parameters. This shows that the phase is indeed a compound and not a solid solution.

Metallographic studies were made to help identify the phases. Polished surfaces of antimony and gadolinium which had been pressed to 50 kilobars and 1000 °C are shown in Figures 12 and 13. The high pressure orthorhombic product is shown in Figure 14 at magnification of 100X and in Figure 15 at 500X. Figure 16 shows a polished surface of the $LaSb_2$ type $GdSb_2$. There is apparently unreacted Sb and Gd in this sample as shown by the light and dark minor constituents. Figure 17 shows a polished surface of the GdSb plus unknown products, type I, reaction region. There are at least three phases present in this sample. From the X ray diffraction intensity data the major phase is probably GdSb.

An electron beam microprobe analysis of the surface shown in Figures 14 and 15 was performed by Advanced Metals Research Corporation of Burlington, Massachusetts. They reported that the globular particles (marked G) in Figure 15 contain 58.7 ± 2 per cent Sb and 41.3 ± 2 per cent Gd. Theoretical for $GdSb_2$ is 60.76 per cent Sb and 39.24 per cent Gd which is within their experimental error. The darker phase (marked D) in Figure 15 was shown to be pure Gd and the lighter phase between the globular particles is

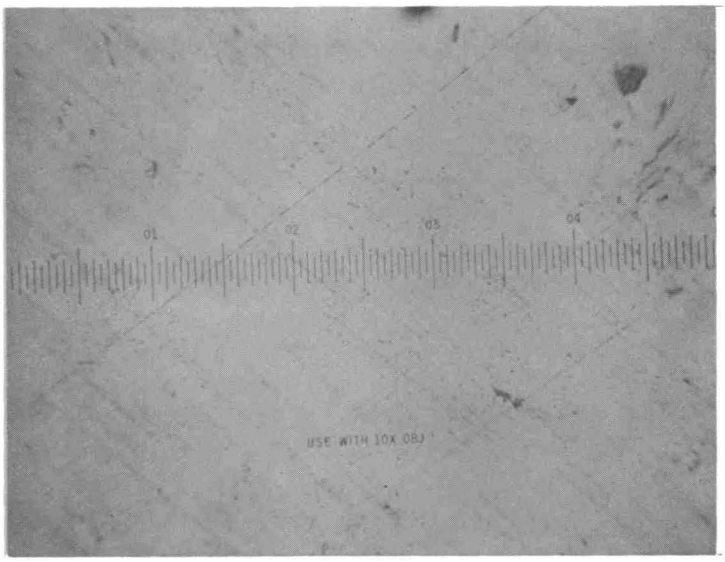

Fig. 12.--Polished Antimony 200X

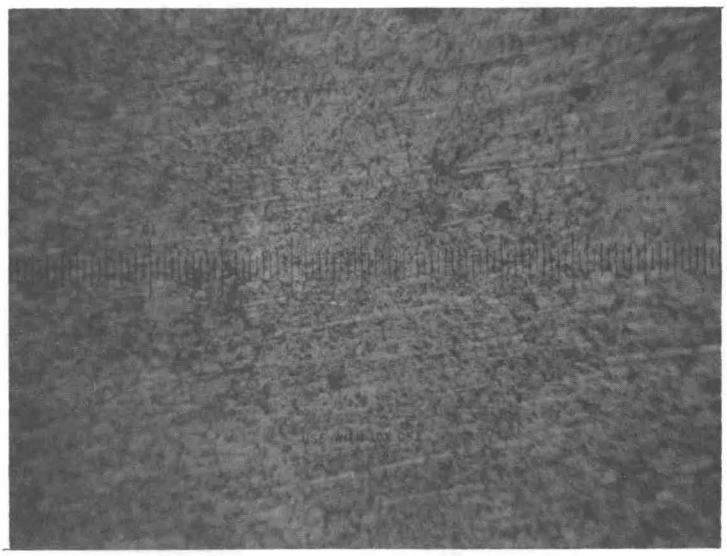

Fig. 13.--Polished Gadolinium 200X

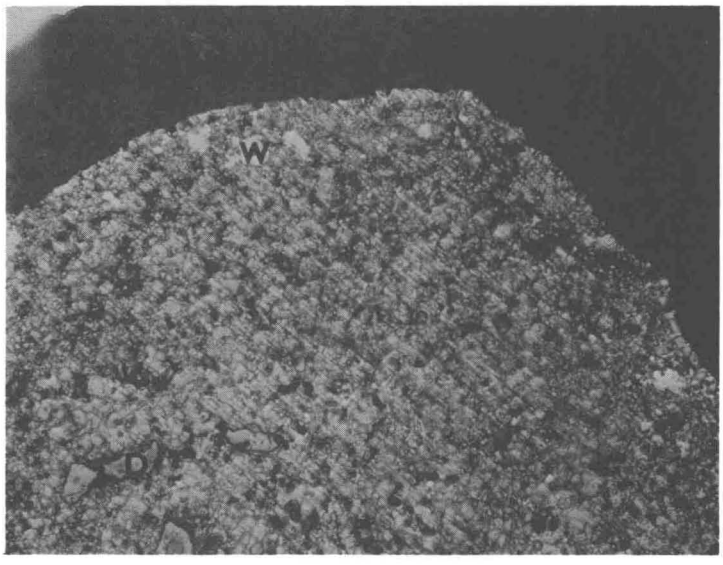

Fig. 14.--Polished High Pressure Orthorhombic $GdSb_2$ 100X

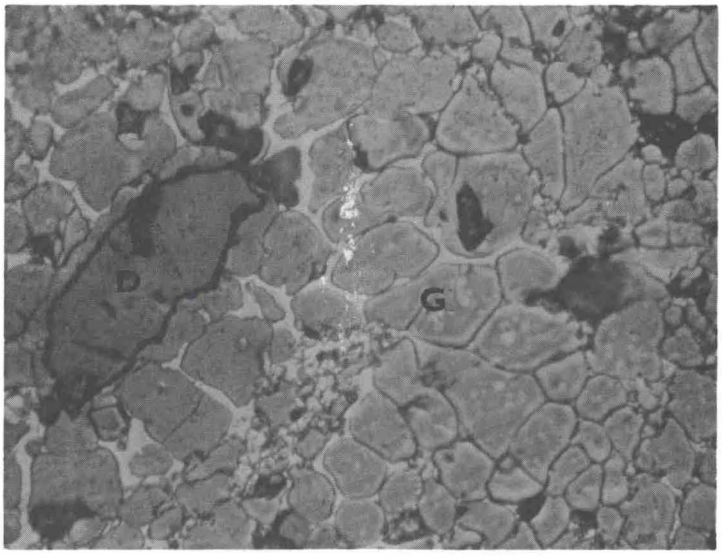

Fig. 15.--Polished High Pressure Orthorhombic $GdSb_2$ 500X

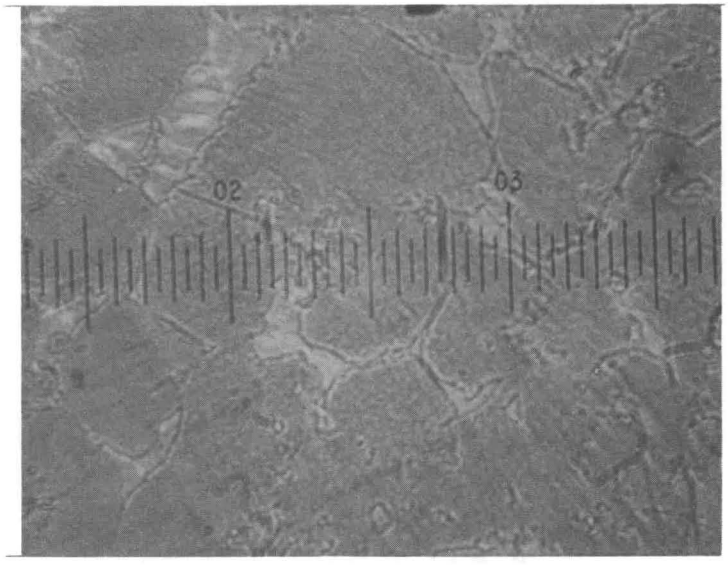

Fig. 16.--Polished $LaSb_2$ Type $GdSb_2$ 400X

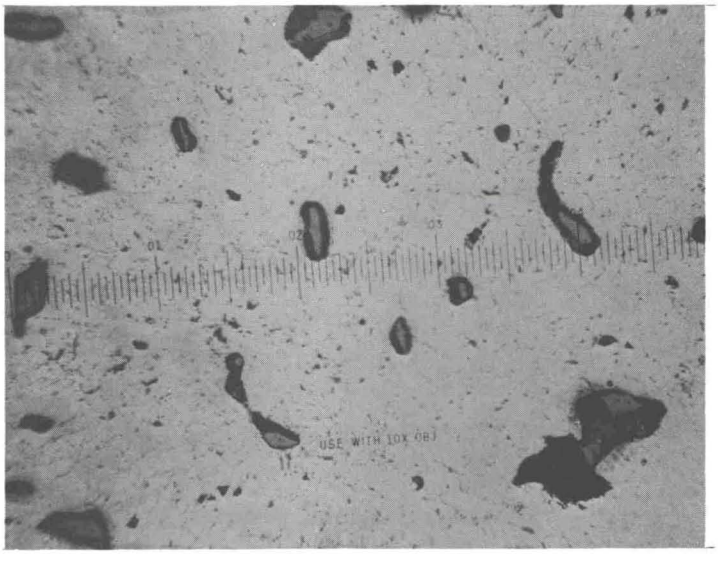

Fig. 17.--Polished GdSb Plus Unknown Substances, Type I, 200X

antimony. The white specks near the edge of Figure 15 (marked W) analyzed approximately 60 per cent Sb, 20 per cent Gd and 20 per cent Mo. The Mo undoubtedly came from the Mo liner used in the metallographic and density runs.

Terbium

At pressures below 30 kilobars and temperatures from 800 to 1500 °C cubic TbSb plus Sb were obtained as found by analysis of the X ray diffraction pattern. At lower temperatures over this pressure range cubic TbSb lines plus a complex pattern analogous to the unknown products, type I, pattern from the Gd plus 2 Sb system were obtained. The $LaSb_2$ type orthorhombic structure characterized by Wang and Steinfink (1) was observed over a narrow pressure band from 35 to 45 kilobars at temperatures from 1100 to 1700 °C. This showed the existence of $TbSb_2$ which was previously unknown. Above 35 to 45 kilobars the high pressure orthorhombic structure observed for $GdSb_2$ was found for all temperatures above 500 °C. $TbSb_2$ exists in two different orthorhombic crystal modifications similar to $GdSb_2$.

At pressures from 30 to 40 kilobars and temperatures above 1400 to 1500 °C only lines from the reactants could be found in the diffraction pattern. Perhaps a compound was formed under these conditions which was not metastable and reverted back to the reactants when the pressure was released.

The reaction product diagram for Tb + 2 Sb is shown

in Figure 6.

Dysprosium

The reaction product diagram for Dy + 2 Sb is shown in figure 7.

At pressures below about 40 kilobars and temperatures above 900 °C cubic DySb plus Sb were obtained. At lower temperatures lines of DySb plus unknown products, type I, were observed. The $LaSb_2$ type orthorhombic structure was not found in this system. The high pressure orthorhombic structure observed in $GdSb_2$ and $TbSb_2$ was obtained at pressures above about 40 kilobars and temperatures above 500 °C. A region where only the reactants were obtained was found at pressures between 40 and 50 kilobars for temperatures above 1700 °C similar to the region found in the Tb + 2 Sb system.

Holmium

The reaction product diagram for Ho + 2 Sb is very similar to that obtained for Dy + 2 Sb and is shown in Figure 8. At pressures below 40 kilobars and temperatures above 700 to 800 °C cubic HoSb plus Sb were obtained. At lower temperatures HoSb plus unknown product, type I, similar to that observed with Gd, Tb and Dy were found. The high pressure orthorhombic phase was observed at pressures above 45 kilobars and temperatures from 500 to about 1700 °C. The region where only reactants were found

was observed from 40 to 60 kilobars above 1600 °C. The $LaSb_2$ type orthorhombic structure was not observed.

Erbium

The reaction product diagram found for the Er + 2 Sb system is shown in Figure 9. Cubic ErSb plus Sb were formed over most of the region investigated. This product was found at pressures below 40 to 60 kilobars depending on the temperature. The ErSb plus unknown product, type I, region was found in a small area from 40 to 50 kilobars at temperatures from 500 to 800 °C. A second complex X ray diffraction pattern was obtained from runs between 50 to 60 kilobars and temperatures from 1200 to 1700 °C. This diffraction pattern was quite different from the lower temperature unknown product, type I, and was not investigated futher. It was called unknown products, type II.

The apparent no reaction region was observed at pressures above 60 kilobars and temperatures above 1600 °C. High pressure orthorhombic $ErSb_2$ was found at pressures above 45 kilobars and temperatures from 500 to 1600 °C. The $LaSb_2$ type orthorhombic structure was not observed.

Thulium

The reaction product diagram found for the Tm + 2 Sb system is shown in Figure 10. As in the case of erbium the cubic TmSb plus Sb phase was found over a broad region of up to 30 to 65 kilobars depending on the temperature.

At pressures up to 30 kilobars the cubic TmSb structure was stable over the entire temperature range investigated. Above 50 kilobars the structure required high temperature to become stable. Between 30 and 55 kilobars the unknown product, type I, diffraction pattern observed along with the cubic rare earth monoantimonide familiar from work with the lighter lanthanides was found from 500 to 800 °C. From 800 to 1000 °C the unknown product, type II, observed at higher temperatures with Er + 2 Sb was found.

The typical high pressure orthorhombic structure was observed at pressures above 50 kilobars and temperatures from about 600 or 700 °C up to the lower temperature limit of the TmSb plus Sb region. A high temperature region of no apparent reaction was not found in this system.

Ytterbium

The only compound found in the Yb + 2 Sb system was the $YbSb_2$ structure already reported by Bodnar and Steinfink (15). The range of investigation covered up to 70 kilobars and 1800 °C.

Lutetium

At all temperatures up to 1800 °C for pressures below 40 kilobars the LuSb plus Sb region was found. Above this pressure the unknown product, type II, like that found at high temperatures in the Er + 2 Sb and Tm + 2 Sb systems was obtained. No other products were found up to 70 kilobars.

Scandium

The only phase found in the Sc + 2 Sb system was ScSb plus Sb over the entire range of pressure and temperature studied which covered up to 70 kilobars and 1800 °C.

Yttrium

The reaction product diagram for the Y + 2 Sb system was very similar to the diagrams obtained for the Dy + 2 Sb and Ho + 2 Sb systems. It is shown in Figure 11.

V. CHEMICAL AND PHYSICAL PROPERTIES OF THE RARE EARTH DIANTIMONIDES

The chemical and physical properties of the $LaSb_2$ type and high pressure orthorhombic rare earth diantimonides are very similar. All the diantimonides are silver-grey, metallic substances whose different phases could not be identified by visual inspection. X ray powder diffraction patterns were required for identification of all runs. Even for the runs where no reaction occurred the products were very similar in appearance to the reacted samples. The product compounds were opaque and quite brittle.

Densities were determined on samples run in Mo tubes. Five or six runs were made and the samples carefully removed from the Mo tubes. From 0.25 to 0.35 gram of material was used and densities were made in a pycnometer with anisole as the fluid displaced. Taking 0.2 milligram as the weighing error the densities had a precision of $\pm$ 2 per cent. Accuracy of the densities was uncertain since the purity of the samples was unknown and the metallographic studies indicated some reactants were still present after the synthesis runs. However, the measured densities correlate quite well with the values published by Wang and Steinfink on pure $LaSb_2$ type compounds (1). Experimental

densities and densities calculated from the lattice parameters are summarized in Table 3 and graphed in Figure 18.

TABLE 3

DENSITIES OF RARE EARTH DIANTIMONIDES

Compound	Experimental Density (gm/cc)	Theoretical Density (gm/cc)
$LaSb_2$ Type		
$LaSb_2$	6.68*	7.02*
$CeSb_2$	6.69*	7.26*
$PrSb_2$	6.90	7.47
$NdSb_2$		7.55
$NdSb_2$	6.82*	7.52*
$SmSb_2$	7.56*	7.83*
$GdSb_2$	7.00	8.10
$TbSb_2$	7.19	8.25
High Pressure Orthorhombic Type		
$GdSb_2$	8.33	8.48
$TbSb_2$	8.47	8.63
$DySb_2$	8.78	8.78
$HoSb_2$	8.74	8.90
$ErSb_2$	8.70	9.00
$TmSb_2$	8.96	9.09
YSb_2	6.92	7.13

* Values taken from Wang and Steinfink (1).

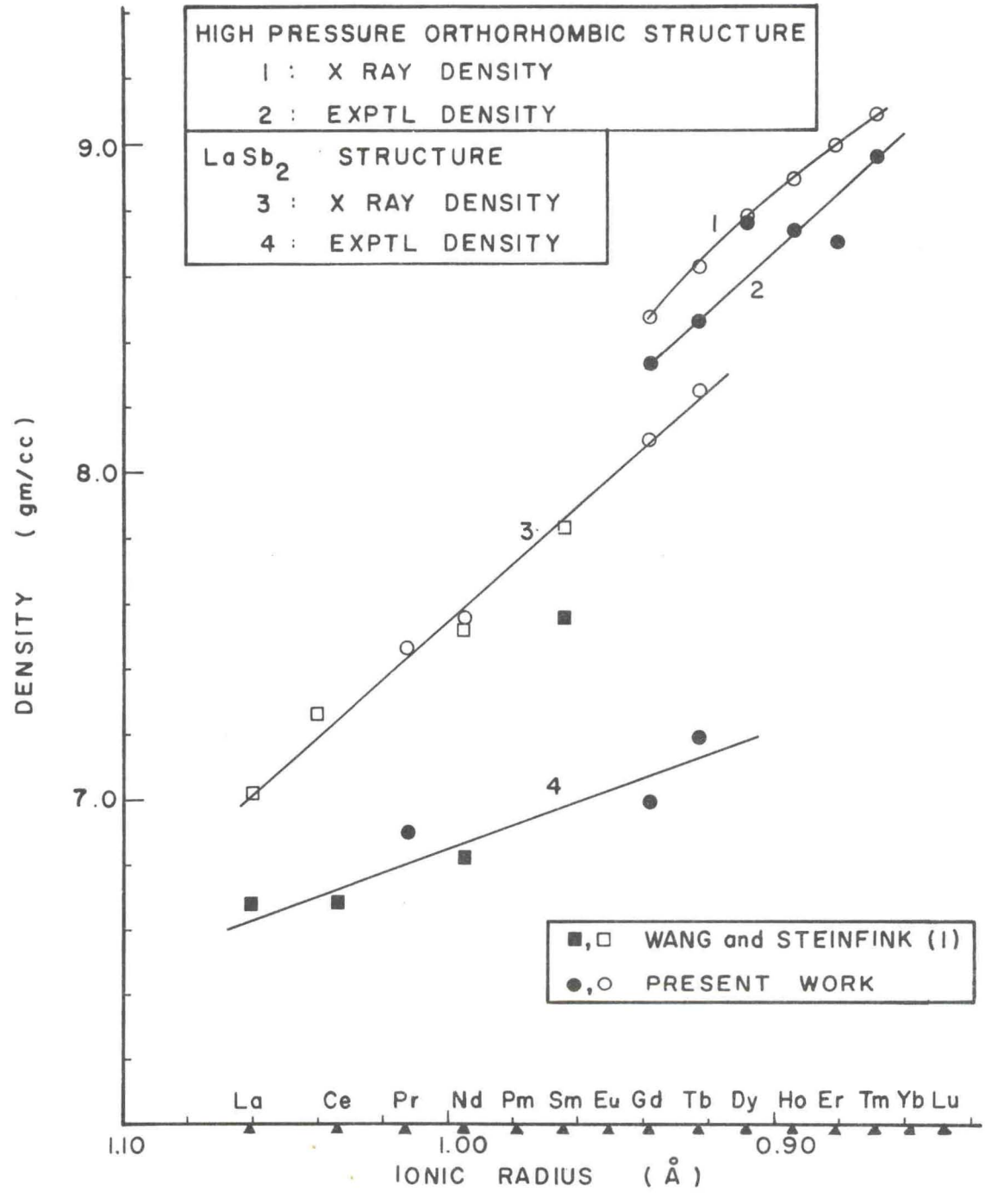

Fig 18.--Densities of Rare Earth Diantimonides.

Chemical reactions of the rare earth diantimonides were found to be very similar. The compounds were treated with one normal solutions of HCl, HNO_3, H_2SO_4 and NH_4OH and with H_2O, acetone, methanol and anisole. No reactions occurred with any of the organic solvents during 24 hours exposure. All diantimonides, including both crystal forms, reacted similarly to the inorganic reagents used. The samples reacted with one normal acid solutions with rapid gas evolution initially which slowed after a few minutes and eventually stopped. After two days the samples were taken to dryness and a metallic residue plus a salt were obtained. The metallic residue was identified as pure antimony in all cases by X ray diffraction analysis. The salts from HCl were mostly pale yellow, from HNO_3 either white or light yellow and from H_2SO_4 either white or colorless. It is presumed that these salts were the salts of the rare earths and the corresponding acid.

All compounds reacted with H_2O and one normal NH_4OH with very slow gas evolution. Residues from these reactions after two days were very similar. X ray diffraction analysis showed antimony metal was present in the residue along with a very complex pattern which was probably the rare earth oxide.

The diantimonides were quite stable when stored in a dessicator or even when exposed to the atmosphere. No decomposition was detected by X ray diffraction analysis

after four months exposure to the atmosphere for high pressure orthorhombic type $HoSb_2$. A sample of $LaSb_2$ type $TbSb_2$ was exposed to the atmosphere initially and then sealed in an X ray cappilary tube and showed no decomposition which could be detected by X ray diffraction analysis after four months.

VI. POLYMORPHISM OF RARE EARTH SESQUISULFIDES

The monoclinic form of Dy_2S_3, Ho_2S_3, Er_2S_3, Tm_2S_3 and Y_2S_3; orthorhombic Yb_2S_3 and rhombohedral Lu_2S_3 were obtained in 95 to 99 per cent purity from K and K Laboratories of Hollywood, California. X ray diffraction patterns were taken on each of these compounds.

Dy_2S_3 was completely converted to the cubic form in the tetrahedral press at 70 kilobars and 1200 °C; however, Dy_2S_3 was already known in both forms. Monoclinic Ho_2S_3 could not be converted to the cubic form at 70 kilobars and 1700 °C which were the maximum conditions attempted in the tetrahedral press. Subsequent runs made in the cubic press at 77 kilobars and about 2000 °C (estimated by the thickness of coesite and kyanite formed in the pyrophyllite) resulted in complete transition to the Th_3P_4 type cubic structure of Ho_2S_3, Er_2S_3, Tm_2S_3, Yb_2S_3 and Y_2S_3. Lu_2S_3 was about 50 per cent changed to the cubic form under these conditions. None of these compounds were known in the cubic form before this study. The crystal structures of the rare earth sesquisulfides are summarized in Table 4.

Migration of BN into the sulfides gave an impure sample and density determinations could not be made. The BN also appeared slightly darkened or yellow after the runs

TABLE 4

SUMMARY OF CRYSTAL FORMS OF KNOWN RARE EARTH SESQUISULFIDES

	Sc	Y	La	Ce	Pr	Nd	Sm	Eu	Gd	Tb	Dy	Ho	Er	Tm	Yb	Lu
α A Ortho-rhombic			26	26	26	26	26	20	26		2				21	
β B Unknown			2	2	2	2										
γ C Cubic		*	2	2	2	2	2		2	6	2;*	*	*	*	*	*
δ D Monoclinic		2									2	6	2	6		
ε E Rhombo-hedral															22	22
ζ Ortho-rhombic	27															

Note:

Numbers indicate prior synthesis (except for Eu_2S_3 which does not exist) and gives the reference as found in the List of References.

Asterisks indicate the structure was synthesized in the present work.

indicating some decomposition may have taken place.

The lattice parameters of the cubic rare earth sesquisulfides are presented in the section on X ray diffraction analysis.

The cubic compounds were found to be good electrical insulators which indicates that they were probably still the R_2S_3 form rather than the R_3S_4 (19).

VII. X RAY DIFFRACTION STUDIES

All runs in the reaction product studies were analyzed by the Debye-Sherrer or powder diffraction method. The samples were ground between two polished tungsten carbide surfaces and loaded in a 0.5 mm glass capillary. Diffraction patterns were obtained on a 143 mm Debye-Sherrer camera with a General Electric CA-7 copper X ray tube using 1.5 to 2 hours exposure. The best films were read on a General Electric Fluoroline illuminator and d values were calculated on the IBM 7040 computer.

The $LaSb_2$ type patterns were indexed by comparing them to the $NdSb_2$ indexing given by Wang (25). Several additional lines were indexed by comparing observed d values with calculated d_{hkl} values using the structure factors given for $NdSb_2$ by Wang and Steinfink (1). The structure factors allowed the selection of the proper d values for the $LaSb_2$ type structure from the list of possible d values calculated from the lattice parameters and Miller indicies. Lattice parameters were calculated by a least squares fit of the observed d values and the assigned Miller indicies. The X ray diffraction data and Miller indicies of the $LaSb_2$ type compounds are given in Table10 in the Appendix.

The high pressure orthorhombic patterns were given an approximate indexing by a computer program for indexing X ray diffraction patterns written at Battelle Northwest (28) and adapted for use on the IBM 7040 by Alan Webb. This program applies the analytical procedure discussed by Azaroff and Buerger (29) in which Miller indicies are assigned to the observed d values by systematic trial and error until a set of indicies can be found which give consistent lattice parameters. For the isometric systems the relation

$$d^2_{hkl} = \frac{a^2}{h^2 + k^2 + l^2} \qquad (1)$$

was used and for the orthorhombic systems the relation

$$\frac{1}{d^2_{hkl}} = \frac{h^2}{a^2} + \frac{k^2}{b^2} + \frac{l^2}{c^2} \qquad (2)$$

was used. In these relations d = interplanar spacing, h,k,l = Miller indicies, and a,b,c = lattice parameters. When the hkl values are successfully assigned to the observed d values so that the lattice parameters calculated from all observed d values are consistent the pattern is said to be indexed.

The high pressure orthorhombic patterns could not be indexed to cubic, hexagonal or tetragonal structures with the above method but several different orthorhombic indexings were possible.

The orthorhombic indexing giving closest to two molecules per unit cell was chosen and refined by trial and

error until the best indexing was obtained consistent with all the patterns. Lattice parameters were calculated by using a least squares analysis of the relation for orthorhombic systems given in equation 2. Then all possible d values were calculated from these lattice parameters using the parameters and the assigned Miller indicies in equation 2. The observed d values were compared to the calculated values and the assigned hkl values were adjusted for best agreement and lattice parameters were recalculated. This procedure was repeated several times until no futher improvement between calculated and observed d values could be obtained. The indexings thus obtained are given in Table 11 in the Appendix.

The cubic Th_3P_4 type patterns obtained in the sesquisulfides were indexed directly from the d values by the method outlined by Azaroff and Buerger (29) using the relation for isometric systems given in equation 1. Lattice parameters were calculated by a least squares analysis of the observed d values and the assigned Miller indicies.

The calculated and observed d values and hkl values for all compounds studied are given in Tables 10, 11 and 12 in the Appendix. The lattice parameters are summarized in Tables 5 and 6. The variation of lattice parameters of the $LaSb_2$ type is shown in Figure 19. Data of Wang and Steinfink are also included (1). The present data seem to fit quite

TABLE 5

LATTICE PARAMETERS OF RARE EARTH DIANTIMONIDES

Diantimonide	a (Å)	b (Å)	c (Å)
$LaSb_2$ Type (8 Molecules/Unit Cell)			
$LaSb_2$*	6.314±.005	6.175±.005	18.56±.01
$CeSb_2$*	6.295±.006	6.124±.006	18.21±.02
$PrSb_2$	6.230±.006	6.063±.006	17.89±.02
$NdSb_2$*	6.207±.004	6.098±.004	18.08±.01
$NdSb_2$	6.230±.004	6.063±.004	17.89±.02
$SmSb_2$*	6.171±.006	6.051±.006	17.89±.02
$GdSb_2$	6.157±.002	5.986±.002	17.83±.01
$TbSb_2$	6.123±.006	5.969±.006	17.72±.02
High Pressure Orthorhombic Type (2 Molecules/Unit Cell)			
$GdSb_2$	5.930±.003	3.296±.002	8.030±.004
$TbSb_2$	5.903±.003	3.282±.002	7.990±.004
$DySb_2$	5.888±.003	3.273±.002	7.965±.004
$HoSb_2$	5.874±.002	3.266±.001	7.939±.003
$ErSb_2$	5.866±.006	3.259±.003	7.926±.008
$TmSb_2$	5.851±.002	3.252±.001	7.912±.004
YSb_2	5.907±.003	3.283±.002	7.981±.004

*Values taken from Wang and Steinfink (1).

TABLE 6

CELL PARAMETERS OF CUBIC RARE EARTH SESQUISULFIDES

Rare Earth Sesquisulfide (4 Molecules/Cell)	a (Å)
La_2S_3	8.731*
Ce_2S_3	8.630*
Pr_2S_3	8.592*
Nd_2S_3	8.527*
Sm_2S_3	8.448*
Gd_2S_3	8.387*
Tb_2S_3	8.32 **
Dy_2S_3	8.292*
Dy_2S_3	8.2991±.0004
Ho_2S_3	8.2650±.0003
Er_2S_3	8.2445±.0003
Tm_2S_3	8.2248±.0005
Yb_2S_3	8.2242±.0004
Lu_2S_3	8.198 ±.002
Sc_2S_3	No known cubic form
Y_2S_3	8.3056±.0006

*Values taken from Picon et al. (2).
**Value taken from Collin and Loriers (6).

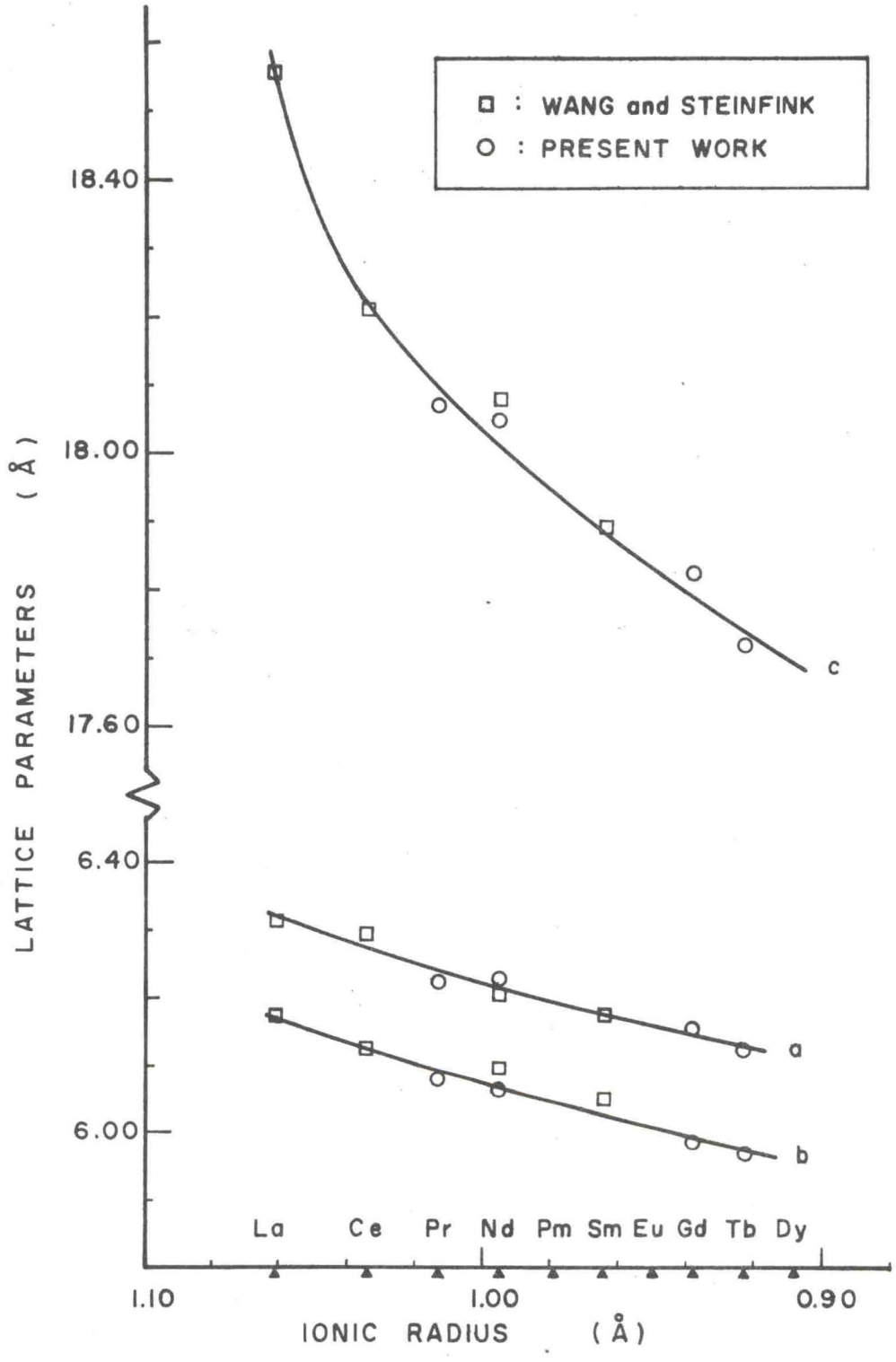

Fig. 19.--Variation of Lattice Parameters With Ionic Radius of $LaSb_2$ Type Rare Earth Diantimonides.

well with the previous work. Ionic radii values were taken from Templeton and Dauben (30).

The shortest Sb-Sb distances in the $LaSb_2$ type compounds were calculated using the atomic positions for $SmSb_2$ from Wang and Steinfink (1) and the lattice parameters in Table 5. The Sb-Sb bond length in antimony metal is 2.90 Å and the shortest Sb-Sb bond reported before Wang and Steinfink's work was 2.81 Å in CdSb and ZnSb (31).

The atomic positions for $SmSb_2$ reported in Wang's dissertation (25) are not the same as those given in the published work by Wang and Steinfink (1). However, the Sb-Sb bond lengths are the same in both works. A check showed the bond lengths were calculated from the atomic positions given in Wang's dissertation. Apparently the atomic positions were refined after the dissertation was written but the bond lengths were not corrected. Corrected bond lengths were calculated from the atomic positions for $SmSb_2$ given in the published work (1) and are different from the values given there for the above reasons. The published and corrected values are summarized in Table 7. Figure 20 shows the variation of the shortest Sb-Sb bond length with ionic radius of the rare earth in the $LaSb_2$ type rare earth diantimonides. It is apparent that the Sb-Sb bond can be as short as 2.76 Å and still be stable or at least metastable. This is 0.14 Å or almost 5 per cent shorter than the bond length in antimony metal which

TABLE 7

Sb-Sb BOND LENGTHS

Compound	Sb-Sb Bond Length (Å)	
Sb (Metal)	2.90	
CdSb, ZnSb	2.81	
$LaSb_2$ Type Rare Earth Diantimonides		
	Published*	Correct**
$LaSb_2$	2.803	2.878
$CeSb_2$	2.760	2.832
$PrSb_2$		2.811
$NdSb_2$		2.806
Nd_3Sb_2	2.742	2.814
$SmSb_2$	2.720	2.788
$GdSb_2$		2.771
$TbSb_2$		2.758

*From Wang and Steinfink (1)
**Calculated from $SmSb_2$ atomic positions from Wang and Steinfink (1) and lattice parameters in Table 5.

represents a considerable compression of the Sb-Sb bond.

The variation of lattice parameters for the high pressure orthorhombic structure is very smooth as shown in Figure 21. The ionic radius of yttrium is usually given as 0.93 Å but it fits at 0.923 Å in the high pressure orthorhombic diantimonide structure and was plotted there.

Cell parameter variation of the Th_3P_4 type rare earth

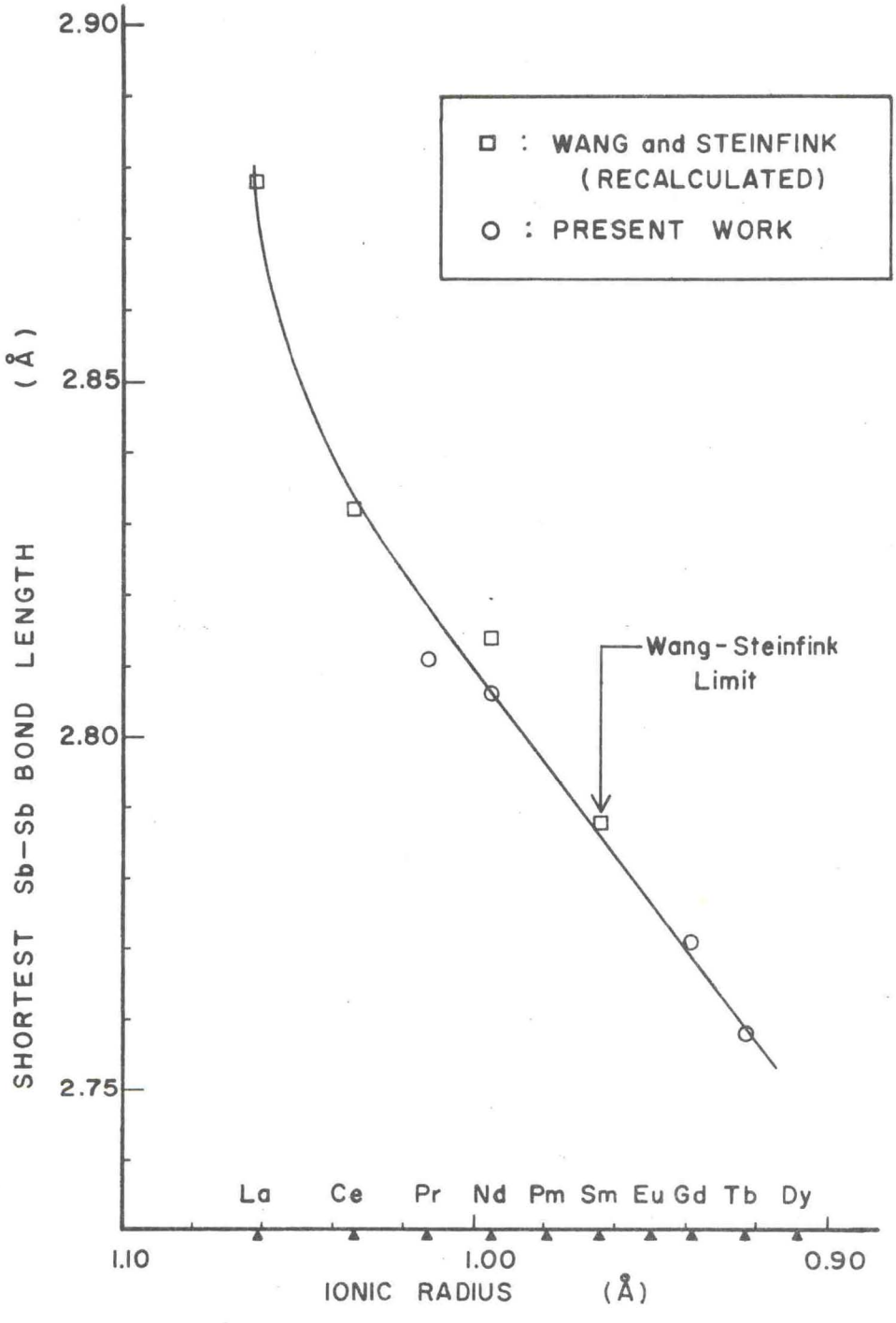

Fig 20.-- Shortest Sb-Sb Bond Lengths in $LaSb_2$ Type Rare Earth Diantimonides.

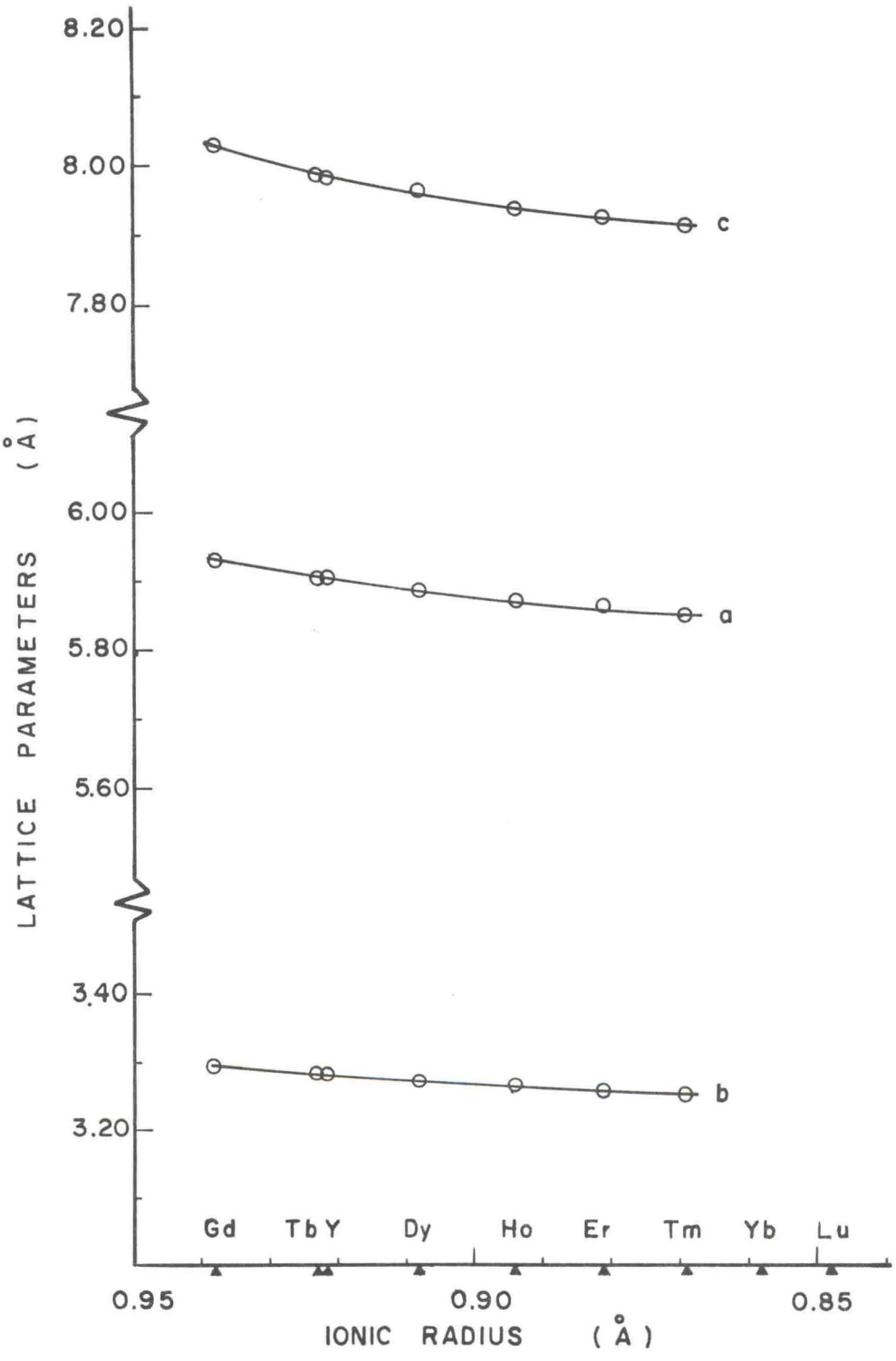

Fig. 21.--Variation of Lattice Parameters With Ionic Radius of High Pressure Orthorhombic Type Rare Earth Diantimonides.

sesquisulfides are shown in Figure 22. Data from Picon and Loriers (2), (6) are also included there. The present work represents a smooth extension of previous work with the exception of Yb which may have some Yb^{++} character.

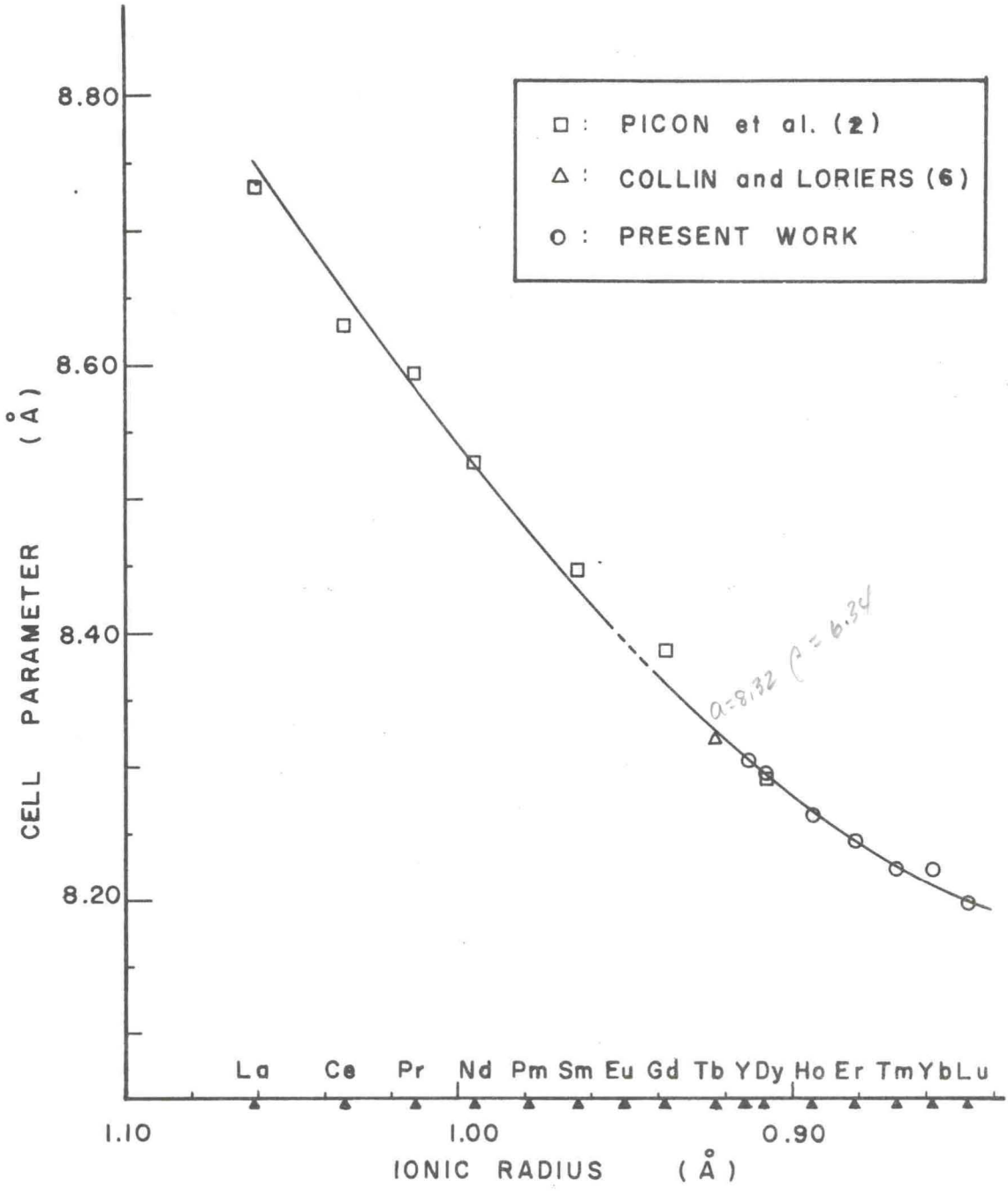

Fig. 22.--Variation of Cell Parameters With Ionic Radius of Rare Earth Sesquisulfides.

VIII. PRESSURE CALIBRATION

As runs were made the oil pressure in the lines to the rams was recorded. This was related to the actual pressure inside the tetrahedrons by calibrating against established transitions.

In all runs the pyrophyllite tetrahedron faces were painted with a slurry of rouge in methanol to increase the friction between the tetrahedron and the anvil face. The tetrahedrons were baked at 110 ^{o}C for at least one hour.

Lees has studied the pressure distribution in the tetrahedron and found about a seven per cent gradient between the centroid and the anvil face and very strong gradients near the gaskets (31). Within one-eighth inch of the centroid the pressure gradient was probably less than one per cent. Since the samples used in this study were generally within one-sixteenth inch of the centroid the pressure gradient over the sample was considered negligible.

In prior calibration studies the relation between oil pressure and sample pressure has been shown to have two regions. Up to 25 kilobars the realtion is an S shaped curve and above 25 kilobars it is quite linear for three-fourth inch anvils (32). Since runs were made above and below 25 kilobars both sections of the curve were

investigated. Two runs were made for each of six transitions and the results are given in Table 7. All runs were made at 25 °C.

TABLE 7

PRESSURE CALIBRATION DATA

Transition	Oil Pressure (psig) Onset	Finish	Transition Pressure (kilobar)	Reference
Ce	580 550	605 575	8.1	(33)
Hg	850 910	860 920	12.2	(34)
Bi I-II	1830 1840	1870 1880	26.5	(35)
Tl II-III	3010 2940	3050 2970	35.4	(35)
Yb I-II	3390 3380		38.2	(35)
Ba I-II	5290 5270	5380 5460	54.6	(35)

The electrical resistance of the sample and oil pressure to the rams were recorded during each pressure calibration run. The transitions were detected by an abrupt change of slope in the resistance versus oil pressure graph. The data for the first run for each transition are shown in Figure 23.

The precision for the pressure calibration data varies from ± 5 psi for the Bi transition to ± 35 psi for

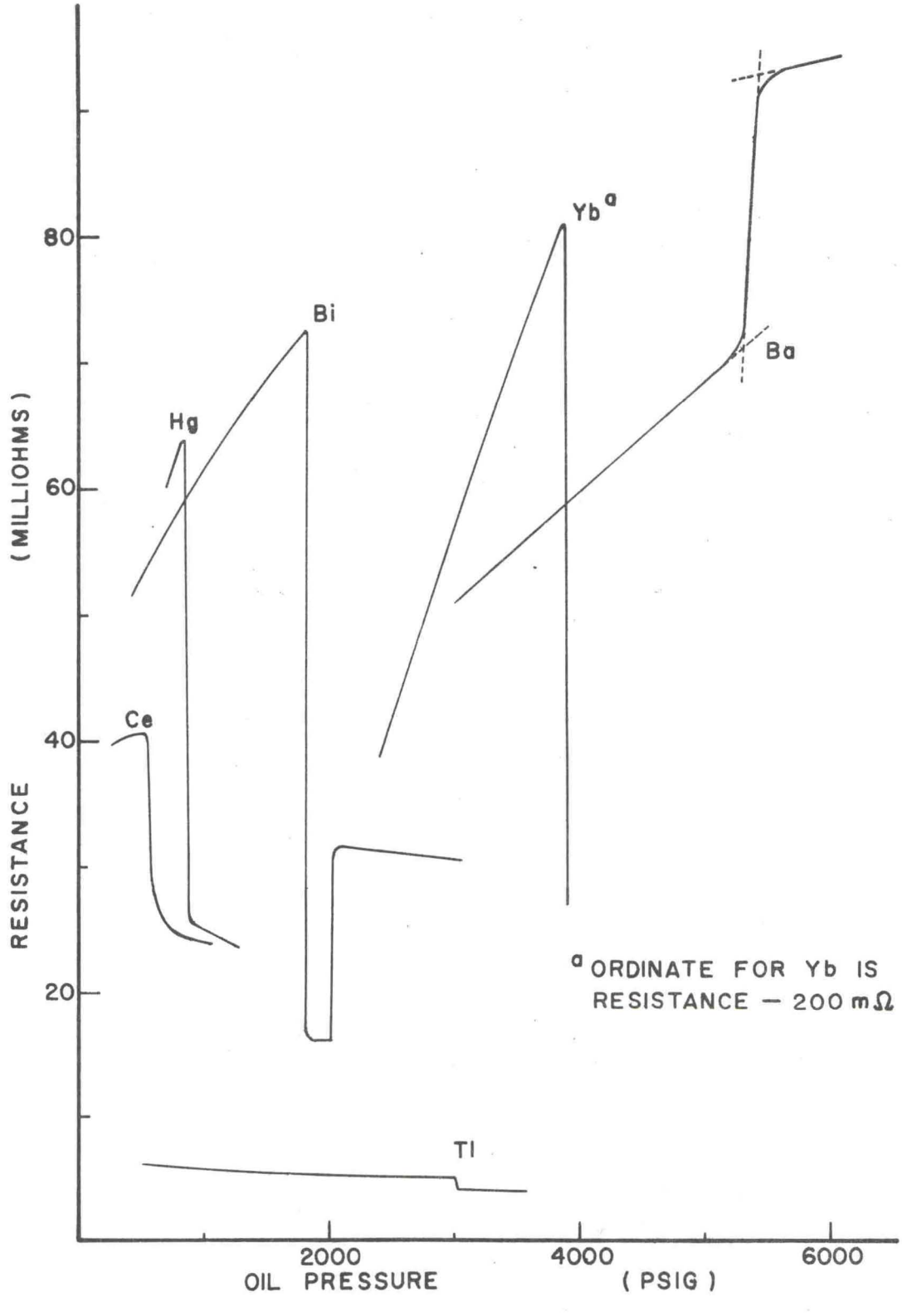

Fig. 23.--Pressure Calibration Transitions.

Tl with an average of ± 15 psi. This corresponds to about ± 0.3 kilobar and pressures seem easily reproducible to within this range.

The oil pressures for onset and finish of the transitions were obtained by straight line extrapolation through the change of slope of the oil pressure versus resistance plot for each transition as shown for the Ba transition in Figure 23. The intersection of the extrapolated straight lines are the values given in Table 8. The Yb transitions were quite sluggish and only onset values were taken for these runs. The averages of the onset values were used to form the pressure calibration plot shown in Figure 24.

For all runs except the Hg transitions the sample consisted of a wire or strip of the metal about 10 mils by 5 mils by 1/4 inch surrounded by AgCl. The AgCl was a cylinder 0.125 inch O.D. by 0.25 inch long with a 0.025 inch hole for the sample. This assembly is shown in Figure 25. Hg could not be contained in this type sample holder and the container was constructed as shown in Figure 26 with the Hg surrounded by boron nitride. The boron nitride was 0.125 inch O.D. by 0.25 inch long in overall dimensions.

Pressure calibration for the runs made on the cubic press were furnished by Dr. H. T. Hall (36).

The effect of temperature on pressure has been

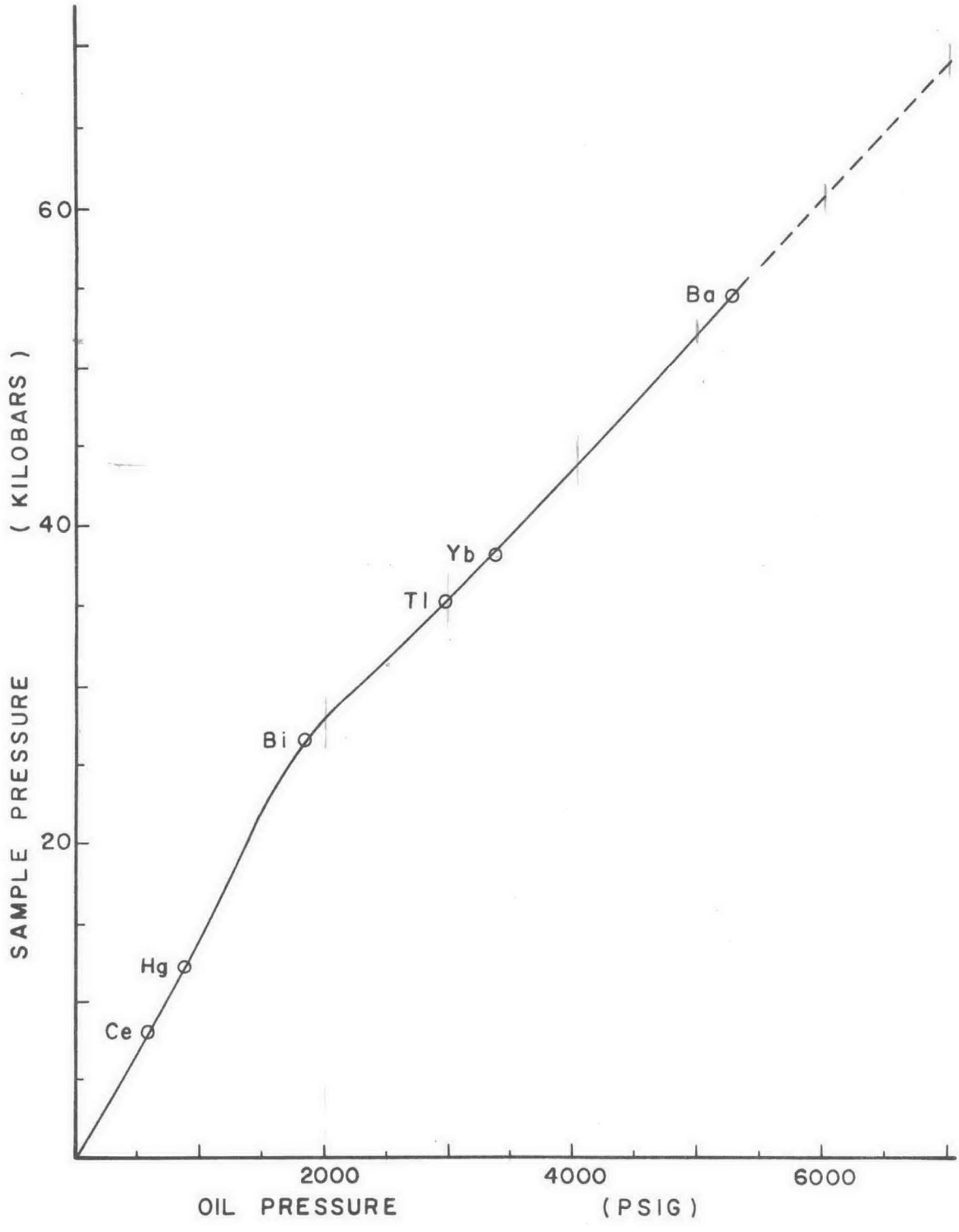

Fig. 24.--Pressure Calibration

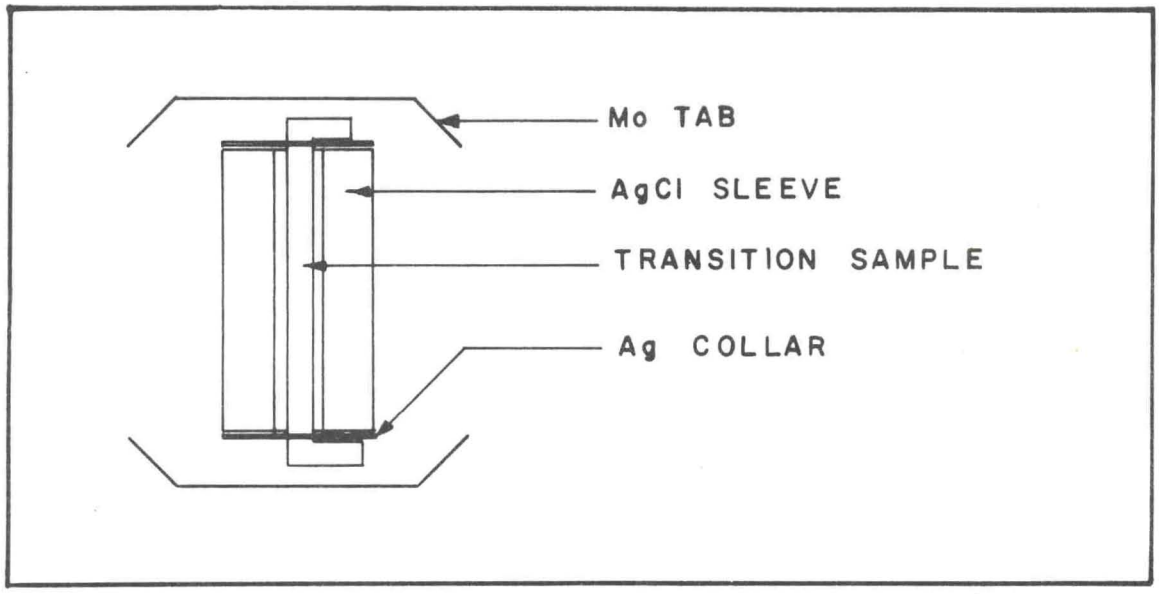

Figure 25.-Pressure Calibration Assembly.

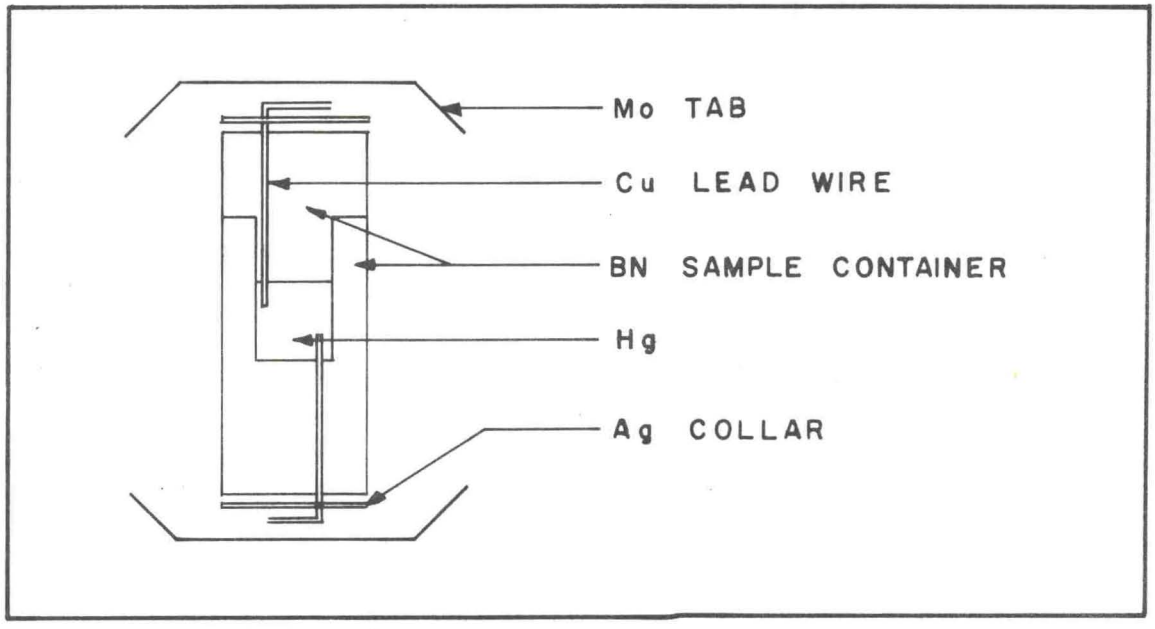

Figure 26.-Pressure Calibration Assembly For Hg Transition.

studied for pyrophyllite cells in carbide anvils. There is probably about 3 to 5 kilobars increase in pressure from heating to 1000 °C at 50 to 70 kilobars over the pressure measured at room temperature (37), (38). This correction is not certain and was not applied to the present studies.

IX. TEMPERATURE CALIBRATION

Each run was heated using the electrical resistance of the graphite heater. The power input was recorded from a wattmeter connected across the anvils.

Fourteen thermocouple runs were made with Pt,Pt-10 per cent Rh thermocouples (butt welded from 10 mil wire) to relate the wattmeter reading to the temperature inside the sample.

In the initial runs it was attempted to insert the thermocouple directly in the rare earth-antimony reaction mixture but the mix dissolved the thermocouple and readings could not be taken this way. It was decided to use a solid BN plug in place of the sample to hold the thermocouple.

Two geometries were used. In the first eight runs the thermocouple wires were taken out the edges of the tetrahedrons and protected by a piece of 0.022 inch O.D. by 0.013 inch I.D. hypodermic tubing 0.75 inch long as shown in figure 27. This arrangement was suggested by Carlson to protect the thermocouple from being broken as the gasket is extruded (37). The thermocouple wires were butt welded and then pulled through the larger hole until the junction bead butted against the BN plug. This made certain that the thermocouple junction was in the center of the sample.

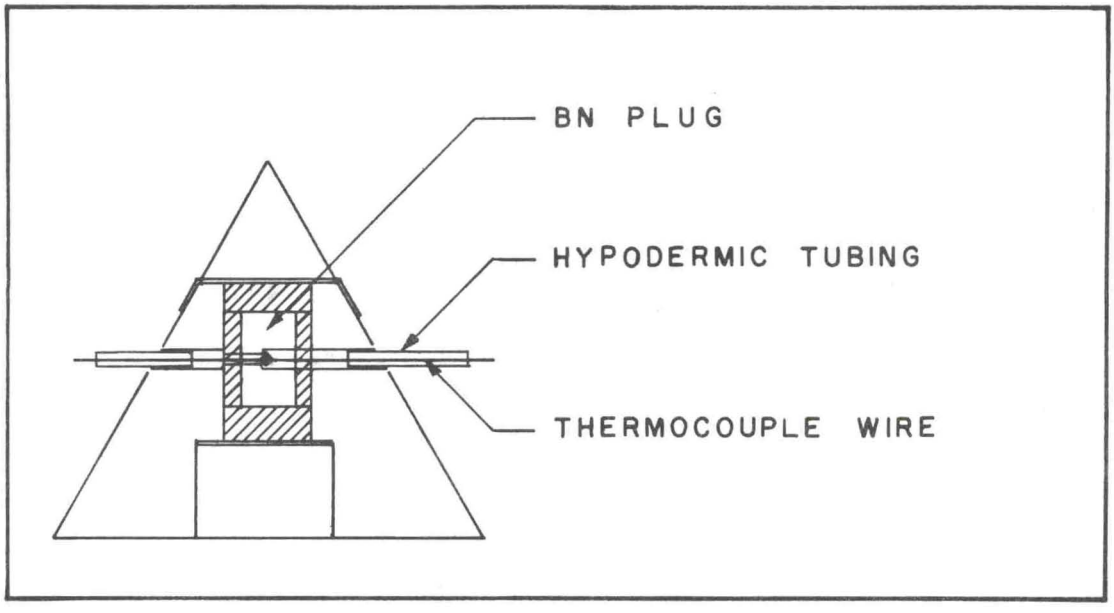

Figure 27.-Temperature Calibration Assembly No. 1.

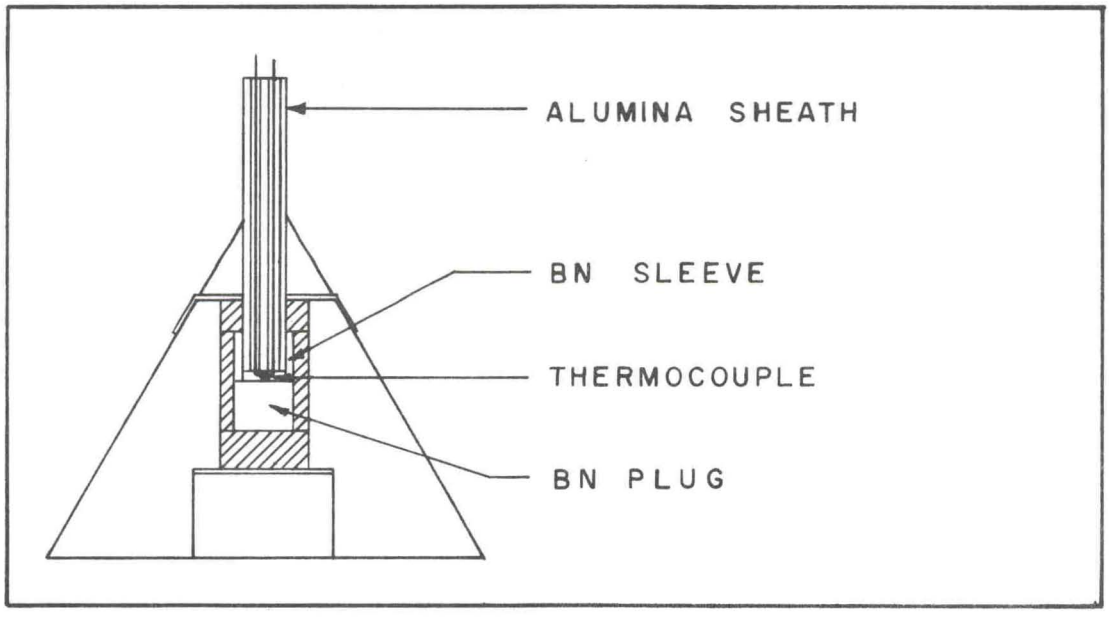

Figure 28.-Temperature Calibration Assembly No. 2.

The larger hole was 0.024 inch in diameter and the small hole was 0.014 inch in diameter. The heater geometry was the same as that used in the synthesis runs and the BN plug was the same size as the BN liners used in the synthesis runs. It was found that if the hypodermic tubes were pushed against the graphite heater they formed a very efficient heat loss path. Their effect is shown in Figure 29. A temperature drop of over 400 °C at 350 watts was noted in two runs where this was done. If the tubing was kept over 0.15 inch away from the heater this effect was not observed. In calibration runs the tubing was inserted 0.20 inch from the heater.

The second geometry was used in runs 9 through 14 and is shown in Figure 28. Both wires were taken out the end of the heater rather than the side and protected by an alumina sheath 0.062 inch O.D. with two 0.012 inch holes for the thermocouple wires. A BN sleeve and plug were used to fill the rest of the graphite heater. Differences between this geometry and the first were within the scatter of the experimental data.

In runs TC-5 and TC-6 a second thermocouple wire was inserted through the BN plug to see if the thermocouple itself was a serious heat sink. The temperatures recorded for these runs were within the scatter of the other runs so this was not considered a serious error. In run TC-6 the second wire was actually from a thermocouple 0.10 inch away

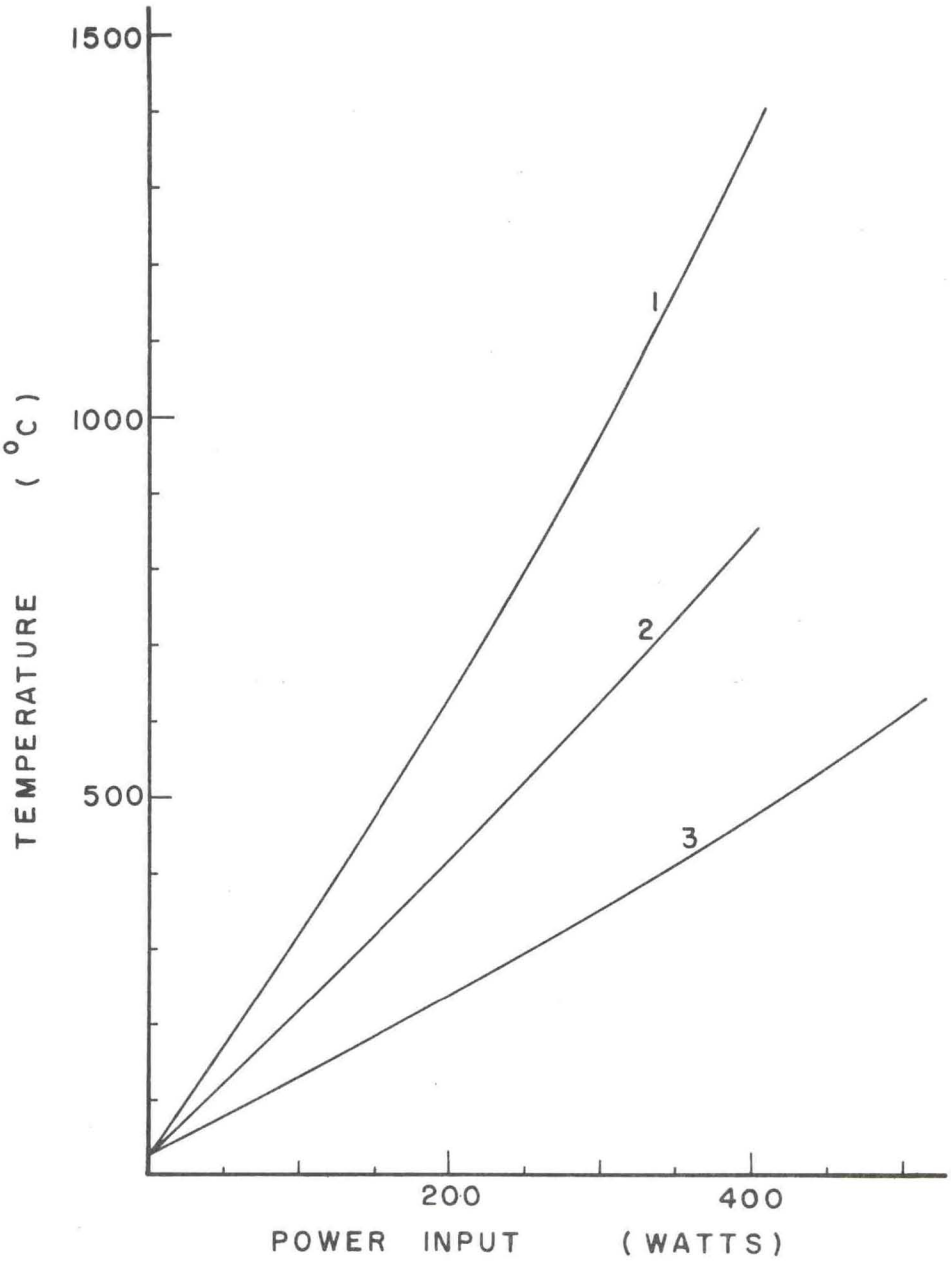

1-Average Temperature Inside Regular Sample
2-Sample Temperature With Hypodermic Tubing Against Graphite Heater
3-Temperature 0.1 Inch Outside Sample

Fig. 29.--Temperature From Inserting Hypodermic Tubing Against The Graphite Heater And Temperature 0.1 Inch Away From Regular Sample.

from the heater in the pyrophyllite. Readings from this thermocouple are shown in Figure 29. It is apparent that there is a very large temperature drop through the pyrophyllite.

All runs made with the geometries shown in Figures 27 and 28 are recorded in Table 9. There is considerable scatter in the data as can be seen from the table. The standard deviation is about * 5 per cent of the temperature over the range measured. Pressure effects of the EMF of Pt-Pt-10 per cent Rh thermocouples have been measured (40), (41) but the corrections are less than the scatter of the data so these corrections were not applied. The average values obtained from all runs are plotted in Figure 30. These values were fitted to quadratic equations by the least squares method and the equations were used to extrapolate to higher values than could be obtained from the actual thermocouple readings. The equations used were:

<u>Oil Pressure</u>

1000 psig $^{\circ}C = 9.3 + 3.374(watts) + 0.0003625(watts)^2$

3000 psig $^{\circ}C = 19.2 + 2.983(watts) + 0.0007060(watts)^2$

5000 psig $^{\circ}C = 40.0 + 2.393(watts) + 0.001763(watts)^2$

7000 psig $^{\circ}C = 54.6 + 2.172(watts) + 0.002042(watts)^2$

The samples were heated by passing alternating current at high amperage, low voltage through the graphite heater. Readings could be obtained from the thermocouples without any AC interference until a temperature at which

TABLE 9

TEMPERATURE CALIBRATION DATA

Power (watts)	Temperature °C					
	TC-1	TC-2	TC-3	TC-4	TC-5	TC-6
1000 psig Oil Pressure						
50	185	200	195	175	165	185
100	350	365	360	345	330	370
150	510	560	535	510	495	560
200	685	720	715	690	655	750
250	850	885	890	885	825	920
3000 psig Oil Pressure						
50	175	190	190	165	155	170
100	330	345	355	320	290	340
150	480	525	530	465	445	500
200	655	680	700	640	600	685
250	805	840	875	800	750	840
300	975	1015	1060	990	925	1040
350	1185	1265	1175	1110	1235	
5000 psig Oil Pressure						
50	170		180	165		
100	315		335	310		
150	455		490	465		
200	615		650	625		
250	760		810	760		
300	925		975	930		
350	1120		1185	1115		
400	1370		1385	1305		
450				1510		
7000 psig Oil Pressure						
50	165		175	160		
100	310		175	160		
150	460		480	445		
200	605		625	585		
250	730		775	730		
300	925		940	890		
350			1130	1060		
400	1285		1335	1240		
450	1500		1545	1435		
500	1735		1750	1635		

TABLE 9

(CONTINUED)

Power (watts)	Temperature °C					
	TC-7	TC-8	TC-9	TC-10	TC-11	TC-12
1000 psig Oil Pressure						
50	185	155	165	180	200	165
100	335	315	335	360	385	325
150	515	480	510	550	575	485
200	685	640	680	740	765	650
250	870	855	925	955	815	890
3000 psig Oil Pressure						
50	165	140	165	175	185	160
100	320	290	315	335	355	295
150	475	435	475	505	530	440
200	630	585	635	680	695	585
250	785	725	785	830	860	735
300	960	895	950	1015	1035	915
350	1170		1125	1200		1095
5000 psig Oil Pressure						
50	160	120	155	150		150
100	305	260	290	315		285
150	450	400	420	470		420
200	595	540	570	630		570
250	750	675	705	780		710
300	905	825	860	955		855
350	1090	1015	1030	1150		1035
400	1290	1205	1215	1360		1220
450		1395	1435	1580		1420
7000 psig Oil Pressure						
50	155	125		160		150
100	295	125		305		285
150	430	390		450		415
200	585	520		605		555
250	725	655		745		685
300	880	805		905		835
350	1060	960		1080		990
400	1275	1135		1280		1175
450	1465	1320		1490		1375
500	1670	1535		1740		1580
550		1765				1785

TABLE 9

(CONTINUED)

Power (watts)	Temperature °C				Per Cent Deviation
	TC-13	TC-14	Average	Standard Deviation	
1000 psig Oil Pressure					
50	180		180	±14	±7.8
100	355		348	±20	±5.8
150	535		525	±30	±5.7
200	710		699	±39	±5.6
250	890		875	±44	±5.0
3000 psig Oil Pressure					
50	170		170	±14	±8.2
100	325		324	±22	±6.8
150	480		483	±33	±6.8
200	650		648	±40	±6.2
250	800		802	±47	±5.9
300	970		980	±51	±5.2
350			1177	±55	±4.7
5000 psig Oil Pressure					
50	155		156	±17	±10.9
100	295		301	±22	±7.3
150	445		446	±28	±6.3
200	595		599	±35	±5.8
250	735		743	±41	±5.5
300	895		903	±49	±5.4
350	1080		1091	±58	±5.3
400	1235		1287	±72	±5.6
450	1485		1471		
7000 psig Oil Pressure					
50		155	156	±14	±9.0
100		295	296	±20	±6.8
150		440	439	±28	±6.4
200		585	583	±33	±5.7
250		735	722	±37	±5.1
300		905	886	±45	±5.2
350		1075	1051	±53	±5.0
400		1250	1247	±64	±5.1
450		1430	1445	±72	±5.0
500		1625	1659	±79	±4.8

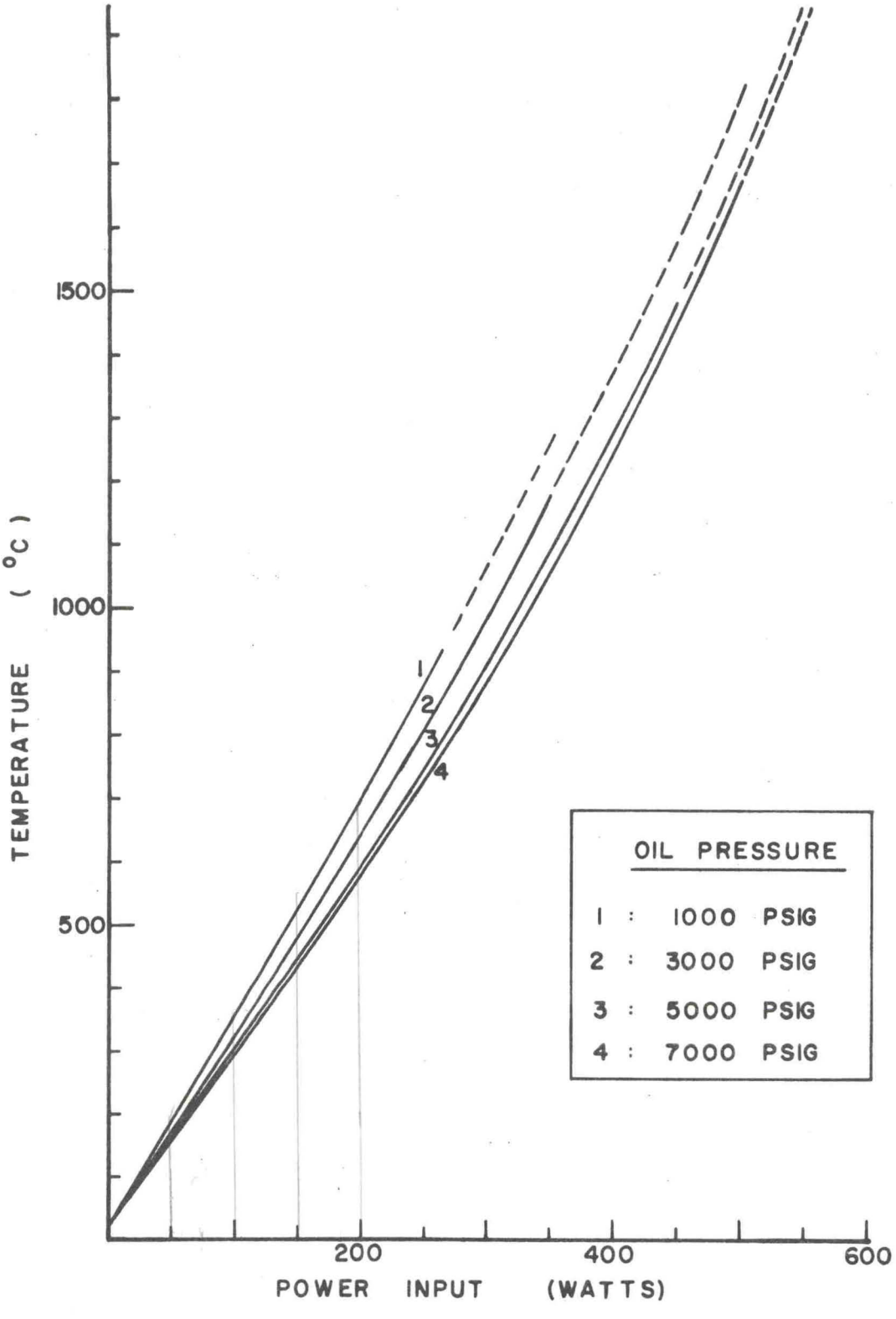

Fig. 30.--Temperature Calibration (Average Values).

the AC interference suddenly became very large. This temperature increased with increasing pressure and in calibration runs readings were taken to within about 50 watts of the upper limit and then stopped.

Run TC-14 was made to see if there was any effect from heating the sample at lower pressures before taking the high pressure readings. As can be seen from Table 9 there seemed to be no effect.

In several runs the heating process was repeated to see if the scatter was high for a given sample. In every case the second temperature readings agreed to within 10 to 15 °C of the initial readings. On one run the temperature was taken both on increasing and decreasing pressure and the agreement was just as good. This shows that a given sample is very consistent and the scatter between different samples must be from differences in sample construction or from differences in the tetrahedrons themselves.

In run TC-4 the power was sustained at 500 watts for 20 minutes after the thermocouple readings were taken and the indicated temperature dropped about 100 °C during this time. There was either considerable thermocouple degradation at these conditions or the formation of coesite and kyanite (high temperature reaction products of the pyrophyllite) results in higher heat transfer out of the sample giving a lower temperature for a given power input.

An estimate of the heating and cooling rates was obtained by connecting the thermocouple output to an oscillograph. At 300 watts steady state was reached in about ten seconds when the sample was taken from room temperature to maximum temperature by sudden application of the power. When the sample was quenched by suddenly turning off the electrical power the temperature dropped to within a few degrees of room temperature in about six seconds.

An interesting result was obtained by measuring the maximum wall thickness of the coesite cylinder which forms around the graphite heater and plotting this thickness against the temperature. The maximum coesite thickness occurs midway between the ends of the cylinder. This correlation is shown in Figure 31 and was used to estimate the temperature of the runs made on the cubic press. All runs in this plot were of three minutes duration. Data from 50 of the synthesis runs are included in the correlation.

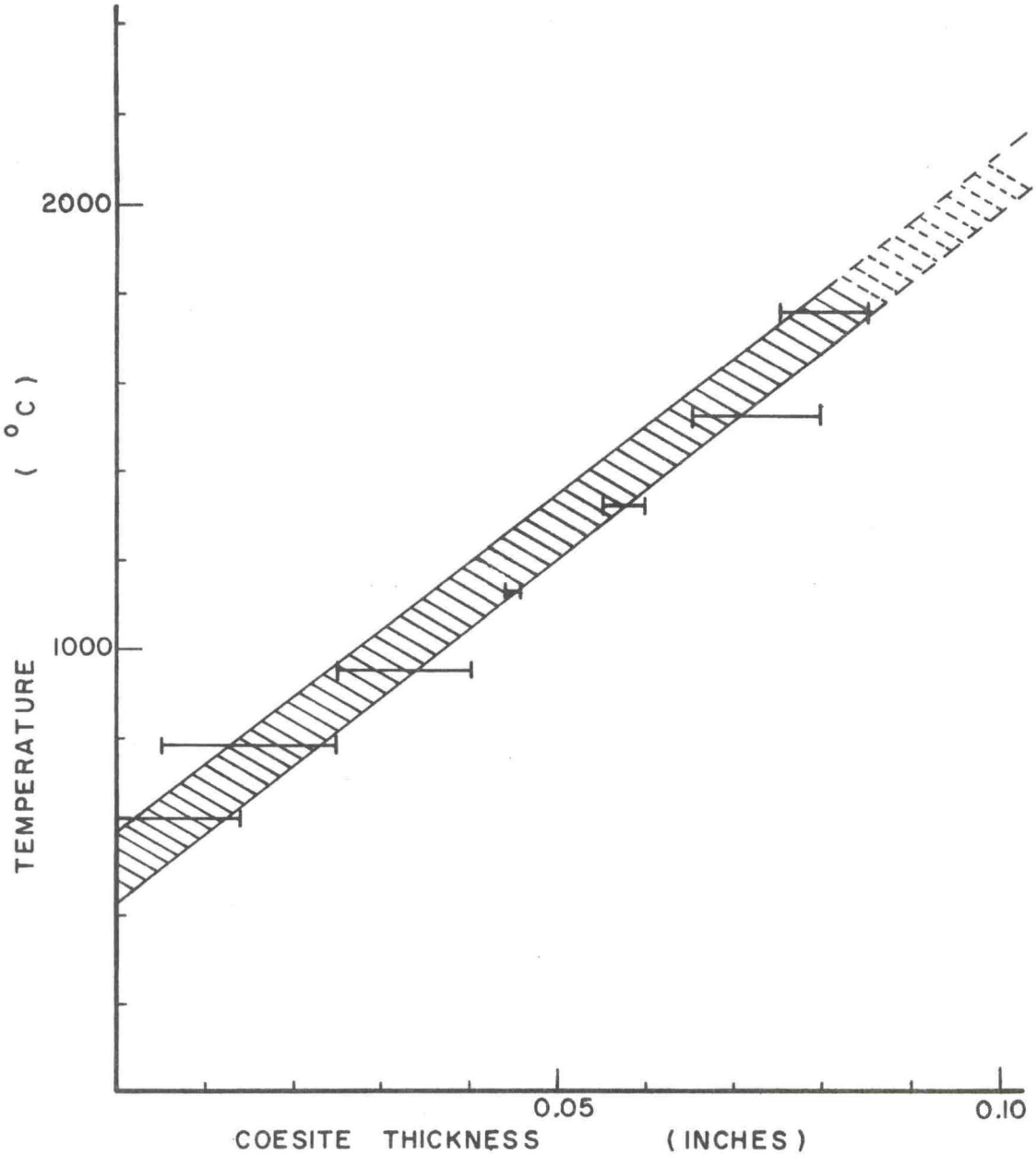

Fig. 31.--Correlation of Coesite Thickness With Sample Temperature. 95 Per Cent Confidence Band is Shown.

X. CONCLUSIONS

The goals of this research were to investigate the rare earth diantimonides to determine if compounds which could not be made by ordinary techniques could be synthesized under high pressure, high temperature conditions and to transform the heavy rare earth sesquisulfides to the cubic form. Both of these goals were accomplished.

A total of eight new compounds were synthesized in the rare earth diantimonides. Besides the eight new compounds eight new polymorphs were made. This shows the powerful applicability of high pressure, high temperature techniques to the field of inorganic synthesis.

Several additional series of rare earth compounds could probably be synthesized using these techniques. The work of Wang and Steinfink (1) suggests that the rare earth diarsenides, disellinides, ditellurides and others might yield additional compounds. In fact, compilations such as "Rare Earth Intermetallic Compounds" by McMasters and Gschneidner (42) have revealed enough incomplete series of rare earth compounds to furnish high pressure workers with almost endless possibilities for productive research.

APPENDIX

TABLE 10

X RAY DIFFRACTION DATA AND INDEXING OF $LaSb_2$ TYPE RARE EARTH DIANTIMONIDES

hkl	Intensity	$PrSb_2$		$NdSb_2$	
		d Obs.	d Calc.	d Obs.	d Calc.
006	vs	3.001	3.011	2.991	3.008
202	m	2.932	2.943	2.915	2.944
023	vvs	2.705	2.713	2.703	2.707
204	m	2.552	2.563	2.543	2.564
116	vw			2.467	2.473
206	vs	2.154	2.164	2.147	2.164
223	vvw	2.047	2.045	2.037	2.043
225	vw	1.859	1.863	1.855	1.861
119	vw	1.823	1.822	1.822	1.821
227	w	1.665	1.663	1.656	1.661
400	vw	1.556	1.556	1.552	1.548
040	vvw	1.521	1.519	1.519	1.518
02,11	vvw			1.442	1.443
406	w	1.381	1.382	1.378	1.383
423	s	1.349	1.350	1.346	1.350
244	vw	1.306	1.307	1.306	1.305
337	vvw	1.264	1.264	1.261	1.263
20,14	vvw	1.194	1.192	1.193	1.182
339	vvw	1.174	1.175	1.170	1.174
00,16	vw	1.130	1.130		
429	vvw			1.137	1.140
440;33,11	vw	1.088	1.087	1.086	1.086
158	w	1.054	1.055	1.053	1.053
446	vvw	1.024	1.022	1.022	1.022
51,10	vvw	1.010	1.011	1.010	1.011
536	vvw	1.001	1.000	1.000	1.000
621	vw	0.980	0.980	0.980	0.981
15,11	vvw	.964	.965	.963	.963
20,18	vw	.956	.955	.955	.947
539	vvw			.936	.938
627	vvw			.916	.918
02,19	vw	.908	.908	.907	.899
60,12	vvw			.854	.854
644	w	.842	.842	.842	.842
718	vw			.822	.820
26,12	w	.811	.811	.810	.810
648	w	0.802	0.801	0.801	0.801

TABLE 10

(CONTINUED)

hkl	Intensity	$GdSb_2$		$TbSb_2$	
		d Obs.	d Calc.	d Obs.	d Calc.
006	vs	2.954	2.971	2.936	2.954
202	m	2.887	2.910	2.877	2.895
023	vvs	2.667	2.673	2.655	2.664
204	m	2.516	2.533	2.506	2.519
116	vw	2.432	2.443	2.423	2.430
117	vvw	2.183	2.190		
206	vs	2.132	2.138	2.119	2.126
223	vvw	2.017	2.018		
312	vvw	1.920	1.897		
225	vw	1.833	1.838	1.829	1.830
119	vw	1.796	1.798	1.785	1.788
227	w	1.641	1.641	1.634	1.633
400	vw	1.536	1.539	1.528	1.531
040	vvw	1.501	1.496		
11,12	vw	1.402	1.404	1.394	1.396
319	vvw	1.386	1.386		
406	w	1.363	1.367	1.365	1.360
423	s	1.333	1.334	1.327	1.328
244	vw	1.291	1.288	1.287	1.284
337	vvw	1.246	1.247		
20,14	vvw	1.178	1.175		
00,16	vw	1.112	1.114	1.108	1.107
156	vvw	1.098	1.093		
440;33,11	vw	1.075	1.073		
158	w	1.039	1.039	1.035	1.036
621	vw	0.969	0.969		
20,18	vw	.943	.943	0.938	0.935
625	vvw	.935	.937		
02,19	vw	.897	.895	.891	.890
60,12	vvw	.845	.844		
644	w	.832	.831	.829	.828
718	vw	.811	.811	.807	.806
26,12	w	.800	.800	.796	.797
648	w	0.791	0.791	0.787	0.788

TABLE 11

X RAY DIFFRACTION DATA AND INDEXING OF HIGH PRESSURE TYPE RARE EARTH DIANTIMONIDES

hkl	Intensity	$GdSb_2$		$TbSb_2$	
		d Obs.	d Calc.	d Obs.	d Calc.
110	vvw	2.899	2.880	2.891	2.869
111	vvs	2.727	2.711	2.717	2.700
003	vw	2.628	2.677	2.621	2.663
112	vvs	2.338	2.340	2.330	2.330
113	vw	1.950	1.961	1.945	1.952
014	vvw			1.708	1.706
310	vvw			1.675	1.688
020	s	1.645	1.648	1.642	1.641
114	s	1.636	1.647	1.628	1.639
021	vvw			1.605	1.608
105	m	1.548	1.550	1.541	1.542
401	m	1.457	1.458	1.451	1.451
221	vvw	1.416	1.418	1.414	1.412
402	w	1.391	1.391	1.385	1.384
106	vvw	1.319	1.305	1.312	1.299
412	vw	1.282	1.281	1.277	1.276
024	vs	1.276	1.274	1.270	1.268
413	vvw	1.202	1.208	1.196	1.201
025	w	1.154	1.150	1.148	1.145
420	vvw	1.101	1.102	1.098	1.097
421	w	1.092	1.092	1.087	1.087
422	w	1.063	1.063	1.058	1.058
316	vw	1.055	1.050	1.050	1.045
026	vvw	1.039	1.039	1.034	1.034
217;423	vvw	1.018	1.018	1.014	1.013
226	w	0.979	0.980	0.974	0.976
034	w	.963	.964	.959	.960
610	vvw	.944	.947	.941	.942
522	vw	.938	.936	.933	.932
523	w	.906	.906	.902	.902
109;431	vvw			.876	.874
417	vw	.873	.875	.870	.870
209	vw	.854	.854	.850	.850
700	vvw			.843	.843
621	vw	.843	.843	.839	.839
622	vw	.830	.829	.826	.826
141	vvw	.810	.812	.807	.809
530	w	.806	.806	.802	.802
712	w	.804	.804	.800	.800
240	w	.794	.794	.791	.791
241;532	w	0.791	0.790	0.787	0.787

TABLE 11

(CONTINUED)

hkl	Intensity	$DySb_2$		$HoSb_2$	
		d Obs.	d Calc.	d Obs.	d Calc.
010	vvw	3.312	3.273		
110	vvw	2.878	2.860	2.877	2.854
111	vvs	2.703	2.692	2.696	2.686
003	vw	2.606	2.655	2.598	2.646
112	vvs	2.320	2.323	2.315	2.317
113	vw	1.938	1.946	1.932	1.941
310	vvw	1.669	1.683	1.666	1.679
020	s	1.636	1.636	1.632	1.633
114	s	1.622	1.634	1.615	1.630
005	m	1.537	1.538	1.534	1.533
401	m	1.448	1.447	1.444	1.444
221	vvw	1.409	1.408	1.404	1.405
402	w	1.380	1.381	1.376	1.377
106	vvw	1.308	1.295	1.303	1.291
412	vw	1.272	1.273	1.269	1.269
024	vs	1.268	1.264	1.263	1.261
413	vvw	1.193	1.198	1.188	1.195
025	w	1.145	1.141	1.142	1.138
420	vvw			1.093	1.092
421	w	1.085	1.084	1.082	1.082
422	w	1.056	1.055	1.052	1.053
316	vw	1.048	1.042	1.043	1.037
026	vvw	1.032	1.031	1.028	1.028
217;423	vvw	1.011	1.010	1.008	1.006
226	w	0.971	0.973	0.969	0.970
034	w	.957	.957	.954	.954
610	vvw	.939	.940	.936	.938
522	vw	.930	.929	.927	.927
523	w	.899	.899	.896	.897
109;431	vvw	.873	.871	.871	.872
417	vw	.867	.868	.865	.866
209	vw	.847	.848	.845	.845
700	vvw	.840	.841	.839	.839
621	vw	.837	.837	.835	.835
622	vw	.823	.823	.822	.821
141	vvw	.804	.806	.803	.804
530	w	.800	.800	.799	.798
712	w	.798	.798	.796	.796
240	w	.788	.788	.787	.787
241;532	w	0.785	0.784	0.783	0.783

TABLE 11

(CONTINUED)

hkl	Intensity	$ErSb_2$		$TmSb_2$	
		d Obs.	d Calc.	d Obs.	d Calc.
011	vvw	3.037	3.014	3.027	3.008
110	vvw	2.863	2.849	2.875	2.842
201	vvw	2.793	2.751	2.770	2.743
111	vvs	2.698	2.681	2.693	2.675
003	vw	2.547	2.642	2.590	2.637
112	vvs	2.315	2.313	2.308	2.308
113	vw	1.930	1.937	1.927	1.933
310	vvw	1.662	1.677	1.662	1.672
020	s	1.631	1.630	1.625	1.626
114	s	1.618	1.627	1.613	1.624
021	vvw	1.597	1.596	1.587	1.593
105	m	1.532	1.530	1.529	1.527
401	m	1.439	1.442	1.439	1.438
221	vvw	1.403	1.402	1.400	1.399
402	w	1.374	1.375	1.370	1.372
106	vvw	1.302	1.289	1.299	1.286
412	vw	1.267	1.267	1.264	1.264
024	vs	1.262	1.259	1.260	1.256
413	vvw	1.187	1.193	1.184	1.190
025	w	1.140	1.136	1.137	1.134
420	vvw	1.091	1.090	1.089	1.087
421	w	1.081	1.080	1.078	1.077
422	w	1.052	1.051	1.049	1.048
316	vw	1.042	1.038	1.040	1.036
026	vvw			1.025	1.024
217;423	vvw	1.007	1.005	1.005	1.003
226	w	0.969	0.969	0.965	0.967
034	w	.953	.953	.951	.951
610	vvw	.935	.936	.932	.934
522	vw	.926	.926	.924	.924
523	w	.895	.896	.893	.894
109;431	vvw	.869	.871	.867	.869
417	vw	.864	.864	.862	.862
209	vw	.844	.843	.842	.842
700	vvw	.837	.838	.835	.836
621	vw	.834	.834	.832	.832
622	vw	.820	.820	.818	.818
141	vvw			.800	.801
530	w	.797	.797	.796	.795
712	w	.794	.795	.793	.793
240	w	.785	.785	.784	.783
241;532	w	0.781	0.781	0.780	0.780

TABLE 11

(CONTINUED)

hkl	Intensity	YSb_2	
		d Obs.	d Calc.
010	vvw	3.269	3.284
110	vvw	2.899	2.870
111	vvs	2.718	2.701
003	vw	2.613	2.660
202	vvw	2.400	2.374
112	vvs	2.335	2.330
113	vw	1.946	1.951
310	vvw	1.678	1.689
020	s	1.641	1.642
114	s	1.627	1.638
005	m	1.543	1.541
401	m	1.453	1.452
402	w	1.384	1.385
106	vvw	1.312	1.298
412	vw	1.278	1.276
024	vs	1.272	1.268
413	vvw	1.196	1.202
025	w	1.149	1.144
421	w	1.090	1.088
422	w	1.060	1.059
316	vw	1.050	1.045
226	w	0.974	0.976
034	w	.960	.960
610	vvw	.942	.943
522	vw	.932	.932
523	w	.902	.902
109;431	vvw	.875	.877
417	vw	.870	.870
209	vw	.849	.849
621	vw	.840	.840
622	vw	.826	.826
530	w	.803	.803
712	w	.800	.801
240	w	.791	.791
241;532	w	0.787	0.787

TABLE 12

X RAY DIFFRACTION DATA OF Th_3P_4 CUBIC TYPE
RARE EARTH SESQUISULFIDES

hkl	Intensity	Observed d Values			
		Dy_2S_3	Ho_2S_3	Er_2S_3	Tm_2S_3
211	vs	3.369	3.382	3.349	3.328
220	vvw		2.924	2.902	2.887
310	vvs	2.610	2.618	2.596	2.589
321	vs	2.208	2.212	2.196	2.189
400	vvw		2.071	2.056	2.050
420	m	1.848	1.851	1.837	1.833
332	w	1.763	1.763	1.754	1.748
422	vvw	1.688	1.688	1.679	1.673
510;431	s	1.624	1.620	1.612	1.608
521	vvw	1.511	1.509	1.502	1.496
440	vvw			1.456	1.449
611;532	s	1.344	1.341	1.334	1.331
620	vw	1.309	1.307	1.301	1.298
541	w	1.279	1.275	1.270	1.266
622	vvw	1.244			
631	vvw			1.212	1.210
444	vw	1.196	1.193	1.188	1.185
640	vw	1.150	1.146	1.141	1.139
721;633;552	s	1.129	1.124	1.121	1.117
642	vvw	1.108	1.104	1.100	1.096
730	vvw	1.089			
732;651	vvw	1.053	1.050	1.046	1.043
653	vw	0.992	0.988	0.985	0.982
822;660	vvw	.964	.961	.972	.968
831;750;743	vw			.958	.955
752	vw	.940	.936	.932	.931
842	vw	.905	.902	.899	.897
921;761;655	w	.894	.891	.888	.886
930;851;754	vw	.875	.871	.868	.867
932;763	vw	.856	.852	.850	.848
10,11;772	vw	.821	.818	.816	.814
950;943	vw	0.806	.803	.801	.799
10,31;952;965	vw		0.788	0.786	0.786

TABLE 12

(CONTINUED)

hkl	Intensity	Observed d Values		
		Yb_2S_3	Lu_2S_3	Y_2S_3
211	vs	3.324	3.311	3.373
220	vvw	2.876		
310	vvs	2.580	2.575	2.614
321	vs	2.187	2.181	2.212
400	vvw	2.046	2.042	
411;330	vvw	1.993		
420	m	1.834	1.820	1.852
332	w	1.743	1.742	1.767
422	vvw	1.672	1.668	1.692
510;431	s	1.611	1.604	1.626
521	vvw	1.497	1.491	1.514
440	vvw	1.450		
611;532	s	1.331	1.326	1.345
620	vw	1.297		1.311
541	w	1.266	1.261	1.280
631	vvw	1.212		
444	vw	1.186		1.197
640	vw	1.139		1.150
721;633;552	s	1.118	1.113	1.129
642	vvw	1.097	1.093	1.110
732;651	vvw	1.043	1.038	1.054
800	vvw	1.026		
653	vw	0.982		
822;660	vvw	.970		
831;750;743	vw	.955	0.951	0.964
752	vw	.930	.926	
842	vw	.897		
921;761;655	w	.886	0.882	.895
930;851;754	vw	.867		.875
932;763	vw	.848		
10,11;772	vw	.814		
950;943	vw	.799		0.807
10,31;952;765	vw	0.784		

LIST OF REFERENCES

1. R. Wang and H. Steinfink, Inorg. Chem., 6, 1685 (1967).
2. M. Picon, L. Domange, J. Flahaut, M. Guittard and M. Patrie, Bull. soc. chim. France, 2, 221 (1960).
3. H. R. Hoekstra, Inorg. Chem., 5, 754 (1966).
4. C. J. M. Rooymans, Chem. Abst., 66, 22966 (1967).
5. V. Stubican and R. Roy, Z. Krist., 119, 90 (1963).
6. G. Collin and J. Loriers, Compt. Rend., 260, 5043 (1965).
7. J. G. White, P. N. Yocom and S. Lerner, Inorg. Chem., 6, 1872 (1967).
8. K. A. Gschneidner Jr., "Crystal Structures of the RM and RM_2 Compounds", Rare Earth Information Center, Ames Laboratory, Iowa State University, Ames, Iowa.
9. L. Brixner, J. Inorg and Nucl. Chem., 15, 199 (1960).
10. G. Bruzzone, A. F. Ruggiero and G. L. Olcese, Chem. Abst., 61, 14021 (1964).
11. M. Przybylska, A. H. Reddoch and G. J. Ritter, J. Am. Chem. Soc., 58, 6437 (1963).
12. A. Iandelli and E. Botti, Chem. Abst., 31, 8301 (1937).
13. R. Vogel and H. Klose, Chem. Abst., 49, 2844 (1955).
14. G. L. Olcese, Chem.Abst., 65, 17877 (1966).
15. R. E. Bodnar and H. Steinfink, Inorg. Chem., 6, 327 (1967).
16. D. Hohnke and E. Parthe, Acta. Cryst., 21, 435 (1966).
17. R. J. Gambino, J. Less Common Metals, 12, 344 (1967).
18. M. Guittard, Compt. Rend., 261, 2109 (1965).

19. M. Cutler, R. L. Fitzpatrick and J. F. Leavy, J. Phys. Chem. Solids, 24, 319 (1963).

20. V. Tien, J. Flahaut and L. Domange, Compt. Rend., 262, 278 (1966).

21. J. Flahaut, L. Domange, M. Patrie and M. Guittard, Compt. Rend., 251, 1517 (1964).

22. J. Flahaut, L. Domange and M. P. Pardo, Compt. Rend. 258, 594 (1964).

23. H. T. Hall, Rev. Sci. Inst., 29, 267 (1958).

24. H. T. Hall, Rev. Sci. Inst., 33, 1278 (1962).

25. R. Wang, PhD Dissertation, University of Texas, 1967.

26. P. Besancon, C. Adolphe and J. Flahaut, Compt. Rend., Acad. Sci. Paris, Ser. C., 266, 111 (1968).

27. J. P. Dismukes and J. G. White, Inorg. Chem., 3, 1220 (1964).

28. J. B. Goebel and A. S. Wilson, "Index, A computer Program For Indexing X-Ray Diffraction Powder Patterns", BNWL-22, Battelle Northwest, Richland, Washington, Jan 1965.

29. L. V. Azaroff and M. J. Buerger, "The Powder Method in X Ray Crystallography", McGraw Hill Book Company, New York, 1958, p. 78 ff.

30. D. H. Templeton and C. H. Dauben, J. Am. Chem. Soc., 76, 5237 (1954).

31. J. C. Slater, "Quantum Theory of Molecules", Vol 2, McGraw Hill, New York, 1965, p. 326.

32. J. Lees, Advances in High Pressure Research, 1, 1-78 (1966).

33. P. W. Bridgeman, Proc. Am. Acad. Arts Sci., 62, 211 (1927).

34. M. K. Zhokhovskii, V. N. Razuminkhin, E. V. Zolotykh and L. L. Burova, Izv. Tech., 11, 26 (1959). Eng. Trans.

35. R. N. Jeffery, J. D. Barnett, H. B. Van Fleet and H. T. Hall, J. Appl. Phys., 37, 3172 (1966).

36. H. T. Hall, personal communication.

37. C. Carlson, PhD Dissertation, Brigham Young University, (1966).

38. H. M. Strong in "Modern Very High Pressure Techniques", ed. by R. H. Wentorf Jr., Butterworths, London, 1962, pp. 97-99.

39. J. Lees and B. H. J. Williamson, Nature, 208, 278 (1965).

40. E. T. Peters and J. J. Ryan, J. Appl. Phys., 37, 933 (1966).

41. R. E. Hanneman and H. M. Strong, J. Appl. Phys., 37, 612 (1966).

42. O. D. McMasters and K. A. Gschneidner Jr., "Rare Earth Intermetallic Compounds", Nuclear Metallurgy Series, 10, 93-158 (1964).